ABSTRACT

Robert W. Privette. PETROLOGY OF THE WEIR SAND (LOWER MISSISSIPPIAN) IN THE ASHLAND-CLARK GAP GAS FIELD OF SOUTHERN WEST VIRGINIA. (Under the direction of Dr. Donald W. Neal) Department of Geology, April, 1983.

The Weir sand is a fine-grained lithic arenite with minor interbedded shales, which was deposited as a marine bar in a delta-front environment. The average composition is 54% quartz, 17% rock fragments, 5% feldspar, 9% carbonates, 7% porosity, 5% matrix, and 3% accessory minerals. The rock fragments include both metamorphic and sedimentary fragments, which indicates a combined metamorphic and sedimentary source area. Porosity includes both intergranular primary and intragranular secondary porosity. The porosity values range from 0 to 13.2% with an average permeability of less than 0.2 md.

Diagenetic changes have affected both the porosity and permeability of the Weir. The greatest effect has been the overall reduction of porosity by compaction and the formation of authigenic minerals, primarily carbonates. Porosity was preserved by the formation of authigenic chlorite, which prevented quartz overgrowth formations during the late stage of diagenesis. Porosity was increased slightly by the creation of secondary porosity due to the dissolution of authigenic minerals and detrital grains.

Diagenetic changes have altered both the porosity and petrology of the Weir. The proposed sequence can be separated in an early, middle, and late stage of diagenesis. The early stage began with the initial

compaction of the sand and the formation of pyrite and pore filling calcite. This was followed by the formation of illite and siderite. The middle stage is characterized by a change in the geochemistry from reducing to oxidizing conditions, the formation of quartz overgrowths, and the creation of secondary porosity. The late stage is characterized by a shift to reducing conditions and the formation of chlorite grain coatings, and a second generation of pore fillings calcite, and the kaolinization of K-feldspar.

PETROLOGY OF THE WEIR SAND (LOWER MISSISSIPPIAN) IN THE ASHLAND-CLARK GAP GAS FIELD OF SOUTHERN WEST VIRGINIA

A Thesis
Presented to
The Faculty of the Department of Geology
East Carolina University

In Partial Fulfillment
of the Requirements for the Degree
Master of Science in Geology

by
Robert W. Privette
April 1983

PETROLOGY OF THE WEIR SAND IN THE ASHLAND-CLARK GAP GAS FIELD IN SOUTHERN WEST VIRGINIA

by

Robert W. Privette

APPROVED BY:

DIRECTOR OF THESIS
Donald W Neal
Dr. Donald W. Neal

COMMITTEE MEMBER
C Q Brown
Dr. Charles Q. Brown

COMMITTEE MEMBER
Scott W. Snyder
Dr. Scott W. Snyder

COMMITTEE MEMBER
Mr. A. Richard Campbell
Consolidated Gas Supply Corp.

CHAIRMAN OF THE DEPARTMENT OF GEOLOGY
C. Q. Brown
Dr. Charles Q. Brown

DEAN OF THE GRADUATE SCHOOL
Joseph G. Boyette
Dr. Joseph G. Boyette

ACKNOWLEDGEMENTS

I would like to express my appreciation to Dr. Donald Neal for guiding the developent of this thesis. I would also like to thank Dr. Scott Snyder and Dr. Charles Q. Brown who served as committee members, and Mr. A. Richard Campbell of Consolidated Gas Supply Corporation for serving as a committee member and for supplying the samples that made this study possible. I also extend thanks to Michael Lyle for his discussions of clay mineralogy.

I want to thank my parents for their support and encouragement, and for making it possible for me to achieve this goal.

This study was partially funded by a grant-in-aid from Sigma Xi, Scientific Research Society.

TABLE OF CONTENTS

TABLE OF CONTENTS (cont'd)

FIGURES

INTRODUCTION

"Weir sand" is the drillers' term for a gas and oil producing zone of the Lower Mississippian Pocono Group in southern and western West Virginia (Fig. 1). The Pocono is defined in the study area (Fig. 2) as the interval between the basal Berea Sandstone and the base of the Maccrady Shale (Fig. 3). Here the Weir is the middle sand unit of the Pocono and is overlain and underlain by intercalated siltstones and shales. The Weir is the subsurface equivalent of the Broadford Sandstone of both the Price Formation in Virginia and the Pocono Group in West Virginia (Reger, 1926). These two sand units are essentially correlative and are differentiated only by geographic and slight lithologic variations (Butts, 1940). The Weir is a fine-grained, lithic sandstone with minor interbedded shales. Bartlett (1974) and Williamson (1974) have described the Weir as a pro-delta deposit.

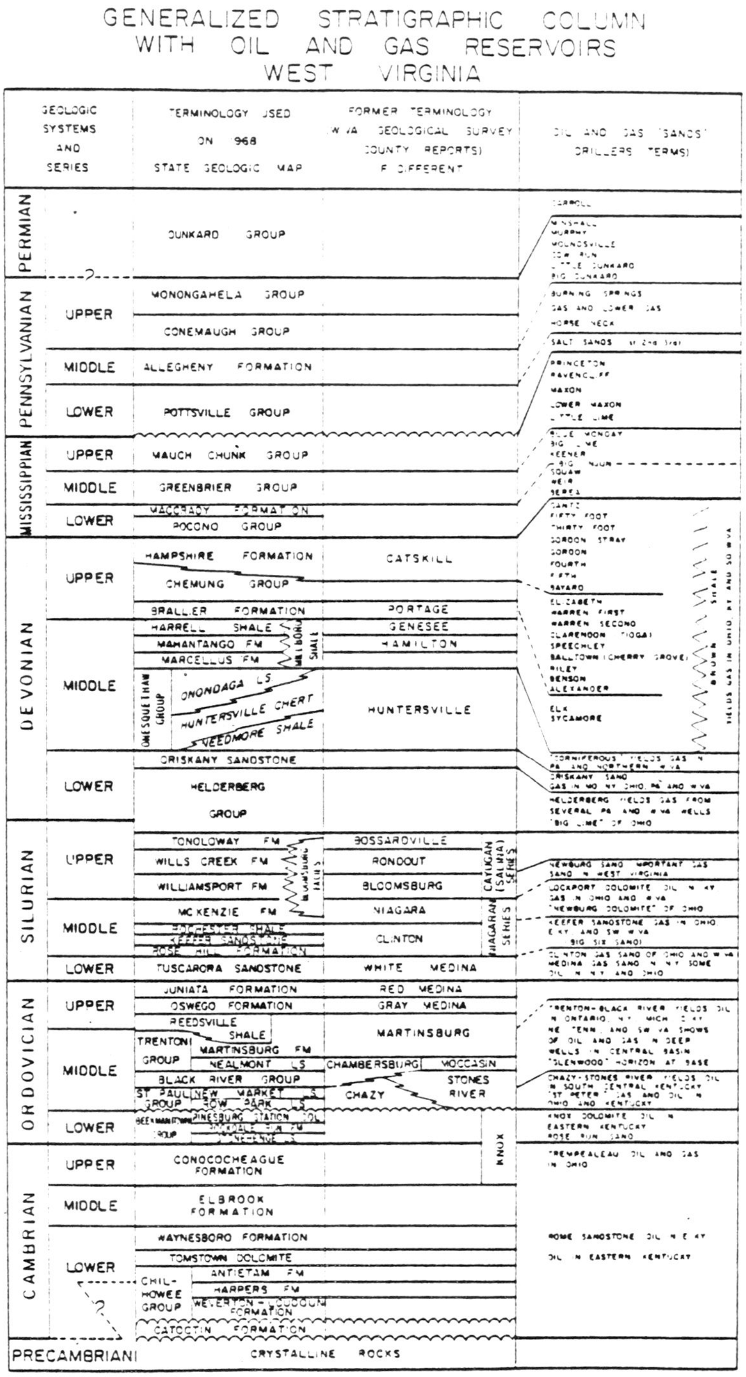

GENERALIZED STRATIGRAPHIC COLUMN
WITH OIL AND GAS RESERVOIRS
WEST VIRGINIA

GEOLOGIC SYSTEMS AND SERIES		TERMINOLOGY USED ON 1968 STATE GEOLOGIC MAP	FORMER TERMINOLOGY (W VA GEOLOGICAL SURVEY COUNTY REPORTS) IF DIFFERENT	OIL AND GAS "SANDS" (DRILLERS TERMS)
PERMIAN	?	DUNKARD GROUP		CARROLL MINSHALL MURPHY MOUNDSVILLE COW RUN LITTLE DUNKARD BIG DUNKARD
PENNSYLVANIAN	UPPER	MONONGAHELA GROUP		BURNING SPRINGS GAS AND LOWER GAS HORSE NECK
		CONEMAUGH GROUP		SALT SANDS (1st 2nd 3rd)
	MIDDLE	ALLEGHENY FORMATION		PRINCETON RAVENCLIFF MAXON
	LOWER	POTTSVILLE GROUP		LOWER MAXON LITTLE LIME
MISSISSIPPIAN	UPPER	MAUCH CHUNK GROUP		BLUE MONDAY BIG LIME KEENER BIG INJUN
	MIDDLE	GREENBRIER GROUP		SQUAW WEIR BEREA
	LOWER	MACCRADY FORMATION POCONO GROUP		GANTZ FIFTY FOOT THIRTY FOOT
DEVONIAN	UPPER	HAMPSHIRE FORMATION	CATSKILL	GORDON STRAY GORDON FOURTH FIFTH BAYARD
		CHEMUNG GROUP		ELIZABETH WARREN FIRST WARREN SECOND CLARENDON (TIOGA) SPEECHLEY BALLTOWN (CHERRY GROVE) RILEY BENSON ALEXANDER ELK SYCAMORE BROWN SHALE FIELDS GAS IN OHIO, KY AND SO W VA
		BRALLIER FORMATION	PORTAGE	
	MIDDLE	HARRELL SHALE (MILLBORO SHALE)	GENESEE	
		MAHANTANGO FM (MILLBORO SHALE)	HAMILTON	
		MARCELLUS FM (MILLBORO SHALE)		
		ONESQUETHAW GROUP: ONONDAGA LS, HUNTERSVILLE CHERT, NEEDMORE SHALE	HUNTERSVILLE	"CORNIFEROUS" FIELDS GAS IN PA AND NORTHERN W VA
	LOWER	ORISKANY SANDSTONE		ORISKANY SAND GAS IN MD NY OHIO, PA AND W VA
		HELDERBERG GROUP		HELDERBERG FIELDS GAS FROM SEVERAL PA AND W VA WELLS "BIG LIME" OF OHIO
SILURIAN	UPPER	TONOLOWAY FM (BLOOMSBURG FACIES)	BOSSARDVILLE (CAYUGAN (SALINA) SERIES)	
		WILLS CREEK FM (BLOOMSBURG FACIES)	RONDOUT (CAYUGAN (SALINA) SERIES)	NEWBURG SAND IMPORTANT GAS SAND IN WEST VIRGINIA
		WILLIAMSPORT FM (BLOOMSBURG FACIES)	BLOOMSBURG (CAYUGAN (SALINA) SERIES)	LOCKPORT DOLOMITE OIL IN KY GAS IN OHIO AND W VA "NEWBURG DOLOMITE" OF OHIO
	MIDDLE	MC KENZIE FM (BLOOMSBURG FACIES)	NIAGARA (NIAGARAN SERIES)	
		ROCHESTER SHALE KEEFER SANDSTONE ROSE HILL FORMATION	CLINTON (NIAGARAN SERIES)	KEEFER SANDSTONE GAS IN OHIO E KY AND SW W VA (BIG SIX SAND)
	LOWER	TUSCARORA SANDSTONE	WHITE MEDINA	CLINTON GAS SAND OF OHIO AND W VA MEDINA GAS SAND IN NY SOME OIL IN NY AND OHIO
ORDOVICIAN	UPPER	JUNIATA FORMATION	RED MEDINA	
		OSWEGO FORMATION	GRAY MEDINA	
		REEDSVILLE SHALE	MARTINSBURG	TRENTON-BLACK RIVER FIELDS OIL IN ONTARIO, NY, MICH, O, KY; NE TENN AND SW VA SHOWS OF OIL AND GAS IN DEEP WELLS IN CENTRAL BASIN "GLENWOOD" HORIZON AT BASE
	MIDDLE	TRENTON GROUP: MARTINSBURG FM, NEALMONT LS	CHAMBERSBURG MOCCASIN	
		BLACK RIVER GROUP	CHAZY STONES RIVER	CHAZY-STONES RIVER FIELDS OIL IN SOUTH CENTRAL KENTUCKY "ST PETER" GAS AND OIL IN OHIO AND KENTUCKY
		ST PAUL GROUP: NEW MARKET LS, ROW PARK LS		
	LOWER	BEEKMANTOWN GROUP: PINESBURG STATION DOL, ROCKDALE RUN FM, STONEHENGE LS	KNOX	KNOX DOLOMITE OIL IN EASTERN KENTUCKY ROSE RUN SAND
CAMBRIAN	UPPER	CONOCOCHEAGUE FORMATION	KNOX	TREMPEALEAU OIL AND GAS IN OHIO
	MIDDLE	ELBROOK FORMATION		
	LOWER	WAYNESBORO FORMATION		ROME SANDSTONE OIL IN E KY
		TOMSTOWN DOLOMITE		OIL IN EASTERN KENTUCKY
		CHILHOWEE GROUP: ANTIETAM FM, HARPERS FM, WEVERTON - LOUDOUN FORMATION		
	?	CATOCTIN FORMATION		
PRECAMBRIAN		CRYSTALLINE ROCKS		

Figure 1. From West Virginia Geologic and Economic Survey.

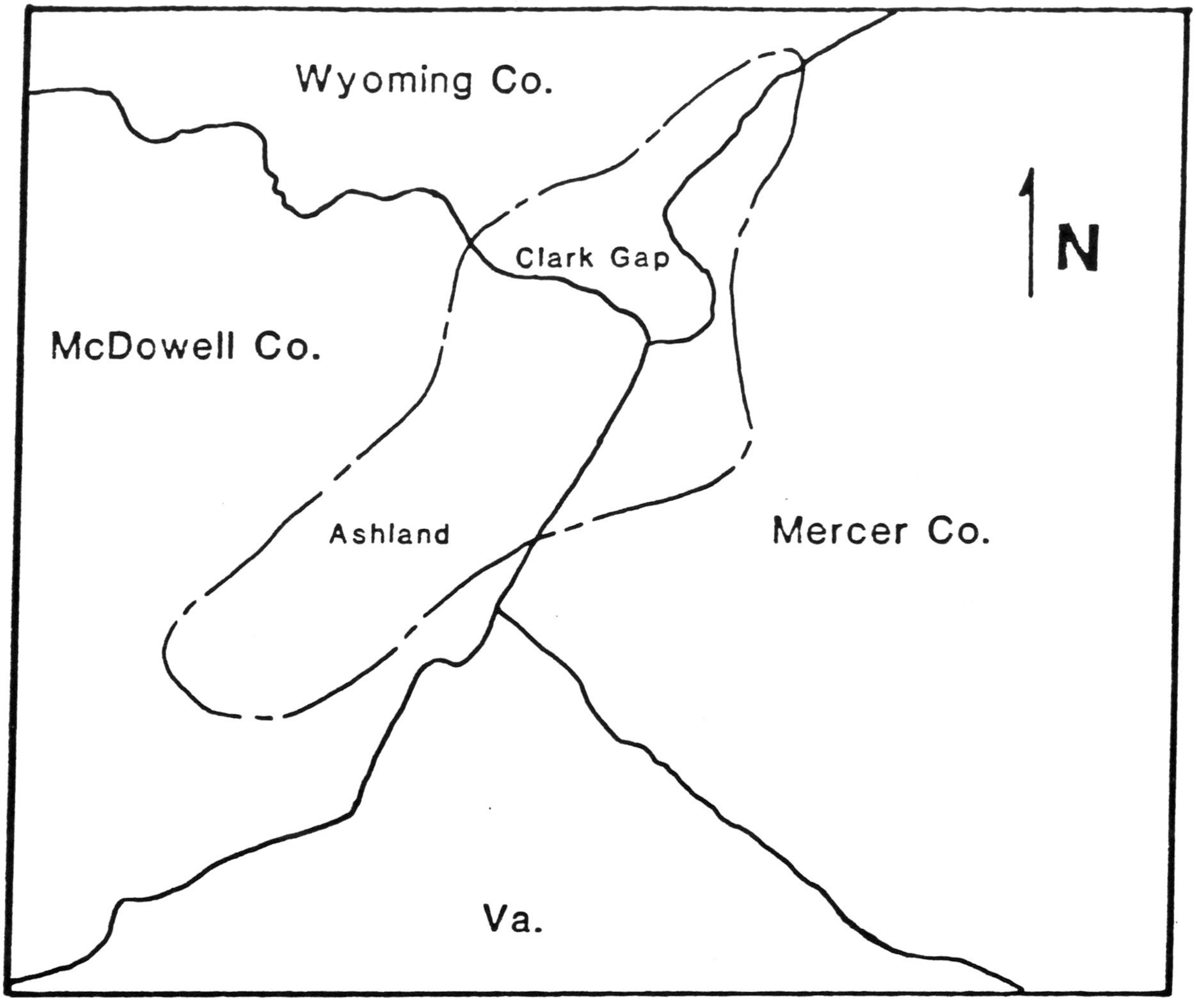

Fig. 2 Study Area

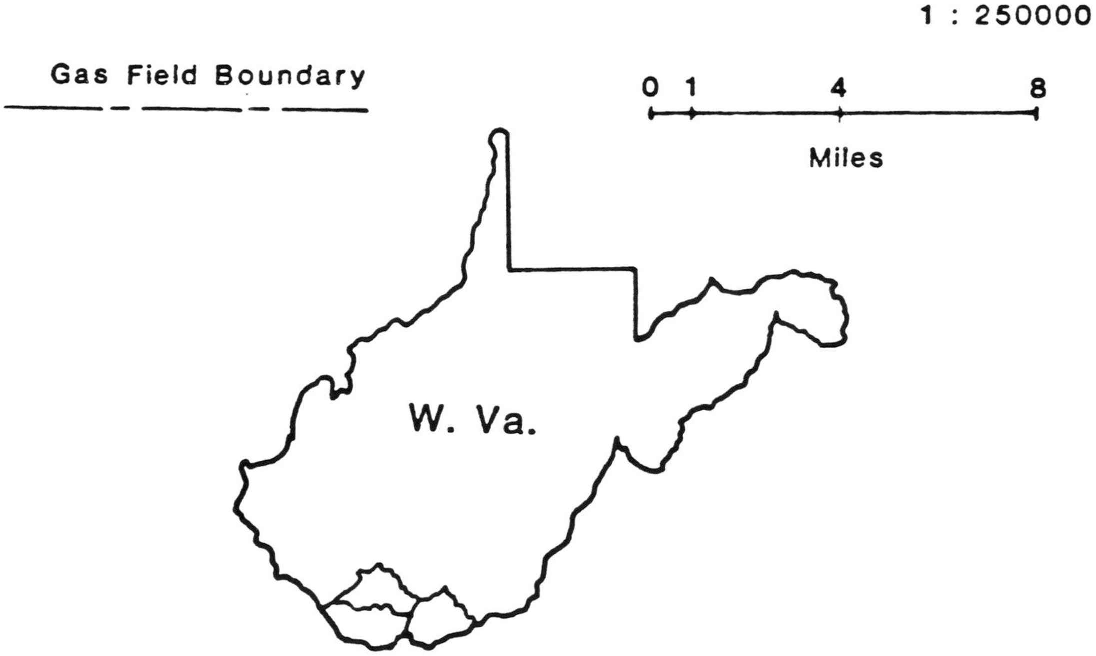

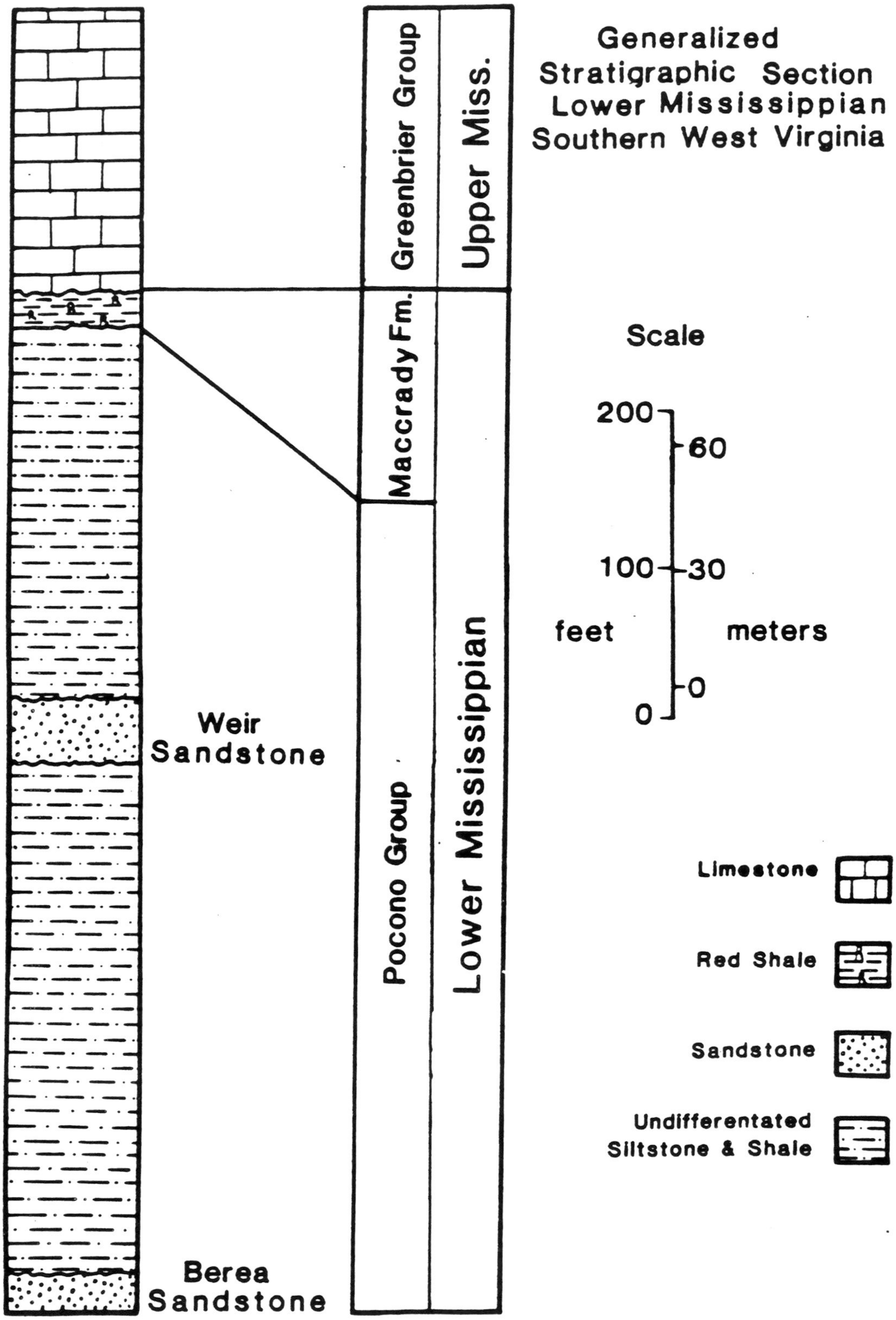
Generalized
Stratigraphic Section
Lower Mississippian
Southern West Virginia
Greenbrier Group
Upper Miss.
Maccrady Fm.
Pocono Group
Lower Mississippian
Weir
Sandstone
Berea
Sandstone
Scale
200
60
100
30
feet
meters
0
0
Limestone
Red Shale
Sandstone
Undifferentated
Siltstone & Shale

Figure 3.

Purpose and Scope

The study is confined to the Ashland-Clark Gap gas field of southern West Virginia. New information on the relationship of petrology to porosity and permeability of the Weir sand may provide a better understanding of factors affecting the production of hydrocarbons and aid in further development of the gas field. The purpose of this study on the Weir sand is threefold: 1) to determine petrographic composition; 2) to describe diagenetic history; and 3) to determine the effects of diagenetic processes on porosity and permeability. The compositional study focuses on authigenic minerals and their relationship to changes in porosity throughout diagenesis.

Geographic Setting

The Ashland-Clark Gap gas field is located in southern West Virginia and covers an area of approximately 125 square miles (325 km^2)in southeastern Wyoming, eastern McDowell, and western Mercer Counties. The area lies on the eastern edge of the Appalachian Plateau physiographic province and is characterized by steep valleys with topographic relief on the order of 800 feet (250 m).

Geologic Setting

The Ashland-Clark Gap gas field is located on the eastern margin of the Appalachian Plateau where strata are generally horizontal. Surface exposures are primarily members of the Pennsylvanian Pottsville Group. No major structural features are found within the study area, but small anticlinal and synclinal features are present. The study area is bordered by larger structures, the Mullins syncline on the northeast and the Abbs Valley and Dry Fork anticlines on the east and southeast.

Subsurface Geology

Subsurface data were derived from gamma-ray wire-line logs on file with the West Virginia Geological and Economic Survey and well locations plotted on the Bramwell, West Virginia-Virginia 15' Quadrangle were supplied by the West Virginia Bureau of Mines. The general profile of the Weir sand, as shown by gamma-ray log profiles, suggests a coarsening-upward sequence of sand with interbedded shales at the base and an abrupt contact with a shale unit at the top. Gamma-ray logs were used to construct an isopach map, a structural contour map, and four cross sections of the Weir in order to relate production trends to structural features or stratigraphic variations within the field. Location of cross sections is shown on Figure 8. Cross section A-A' (Figure 4) shows the Weir thins from northeast to southwest. Cross section B-B' (Figure 5) shows the Weir thins to the southeast and east. Figure 6, cross section C-C', also shows thinning to the southeast and Figure 7,

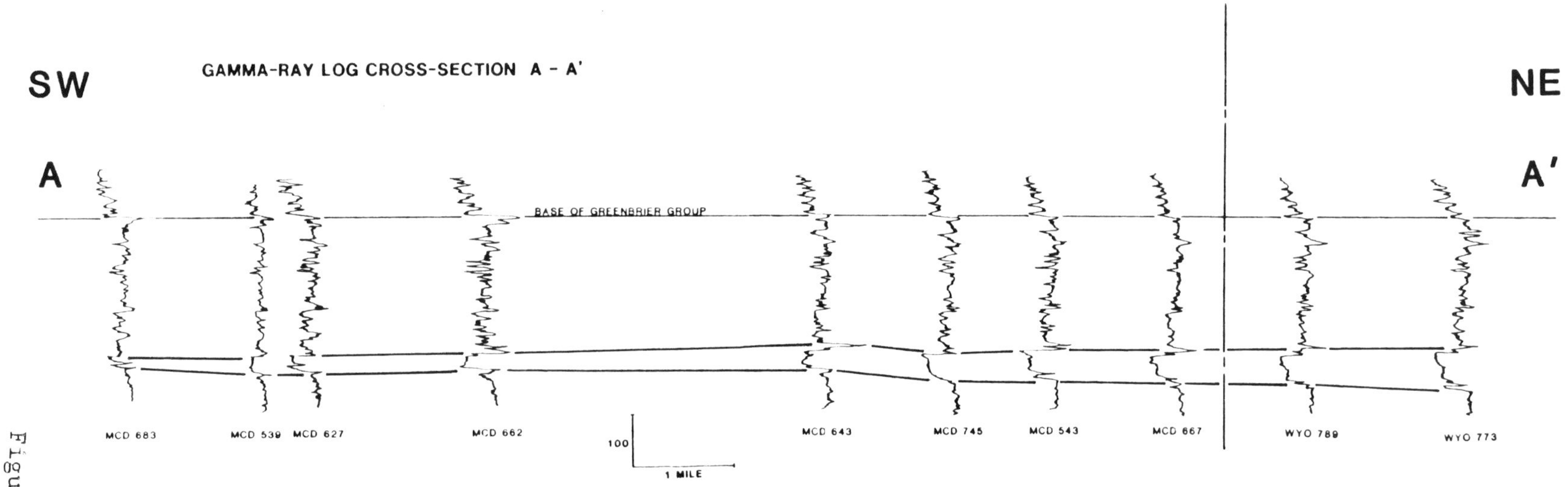
GAMMA-RAY LOG CROSS-SECTION A - A'

Figure 4.

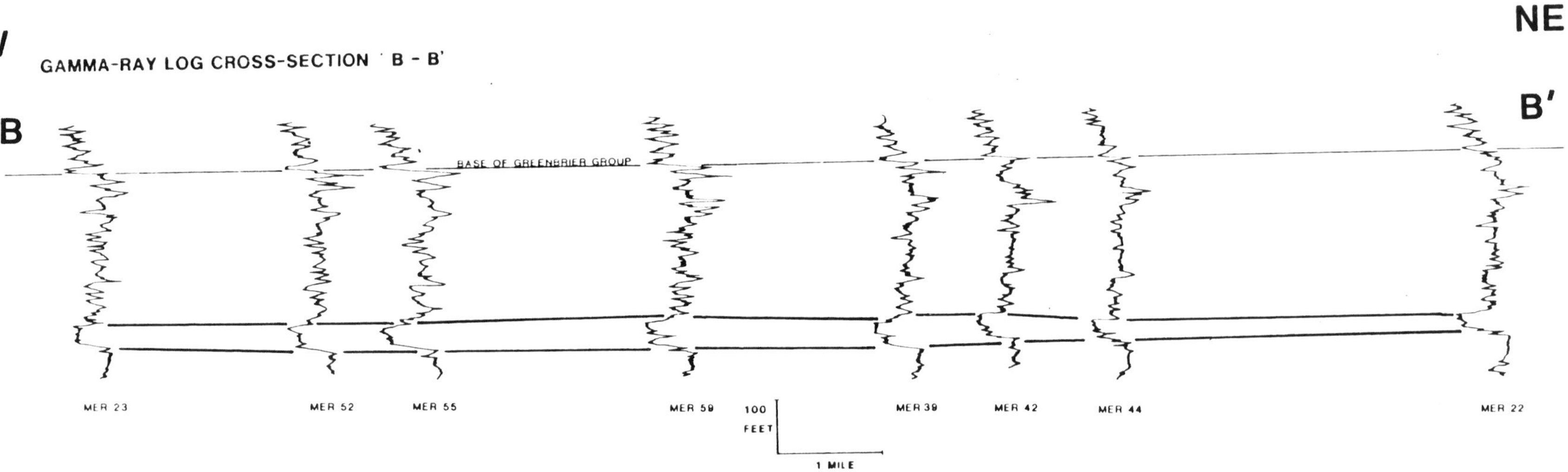
SW
GAMMA-RAY LOG CROSS-SECTION B - B'
NE
B
B'
BASE OF GREENBRIER GROUP
MER 23
MER 52
MER 55
MER 59
100 FEET
1 MILE
MER 39
MER 42
MER 44
MER 22

Figure 5.

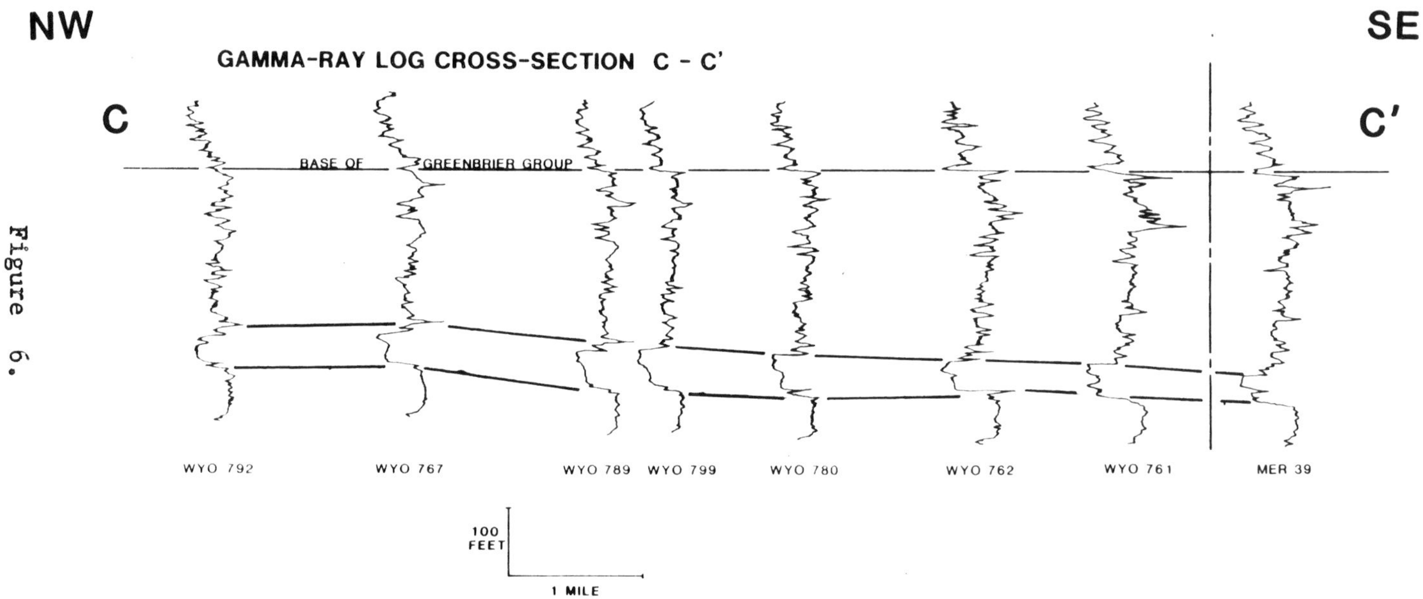
NW
SE
GAMMA-RAY LOG CROSS-SECTION C - C'
C
C'
BASE OF GREENBRIER GROUP
WYO 792
WYO 767
WYO 789
WYO 799
WYO 780
WYO 762
WYO 761
MER 39
100 FEET
1 MILE

Figure 6.

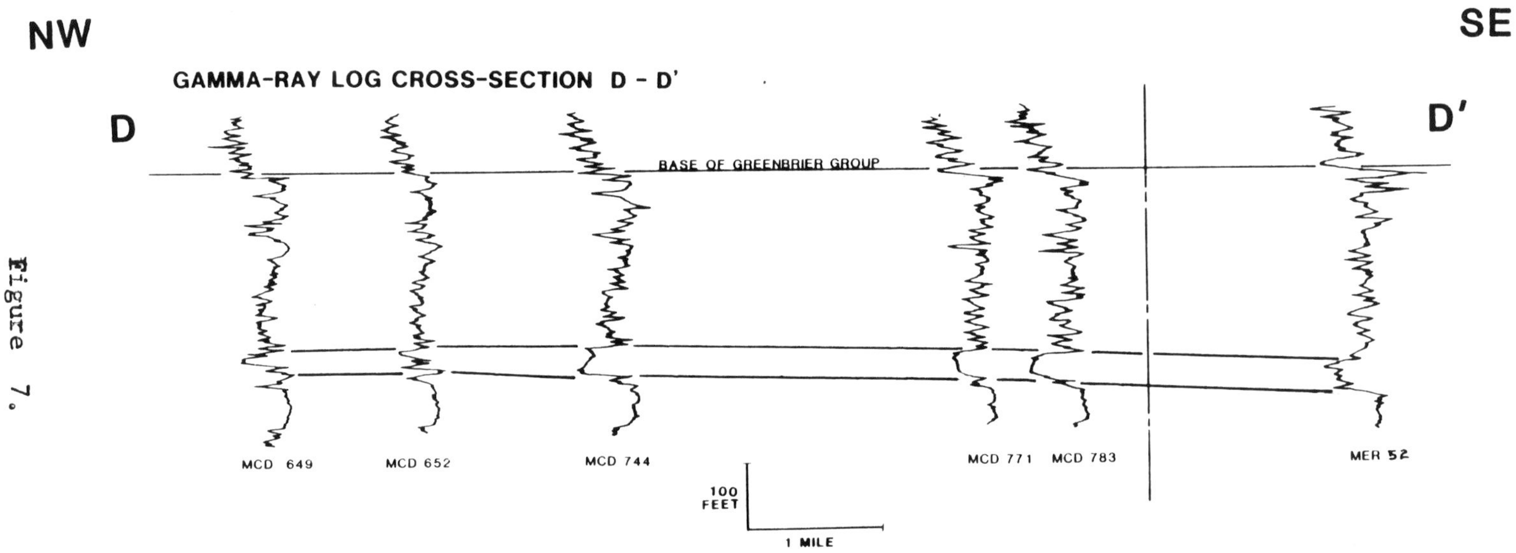
NW
SE
GAMMA-RAY LOG CROSS-SECTION D - D'
D
D'
BASE OF GREENBRIER GROUP
MCD 649
MCD 652
MCD 744
MCD 771
MCD 783
MER 52
100 FEET
1 MILE

Figure 7.

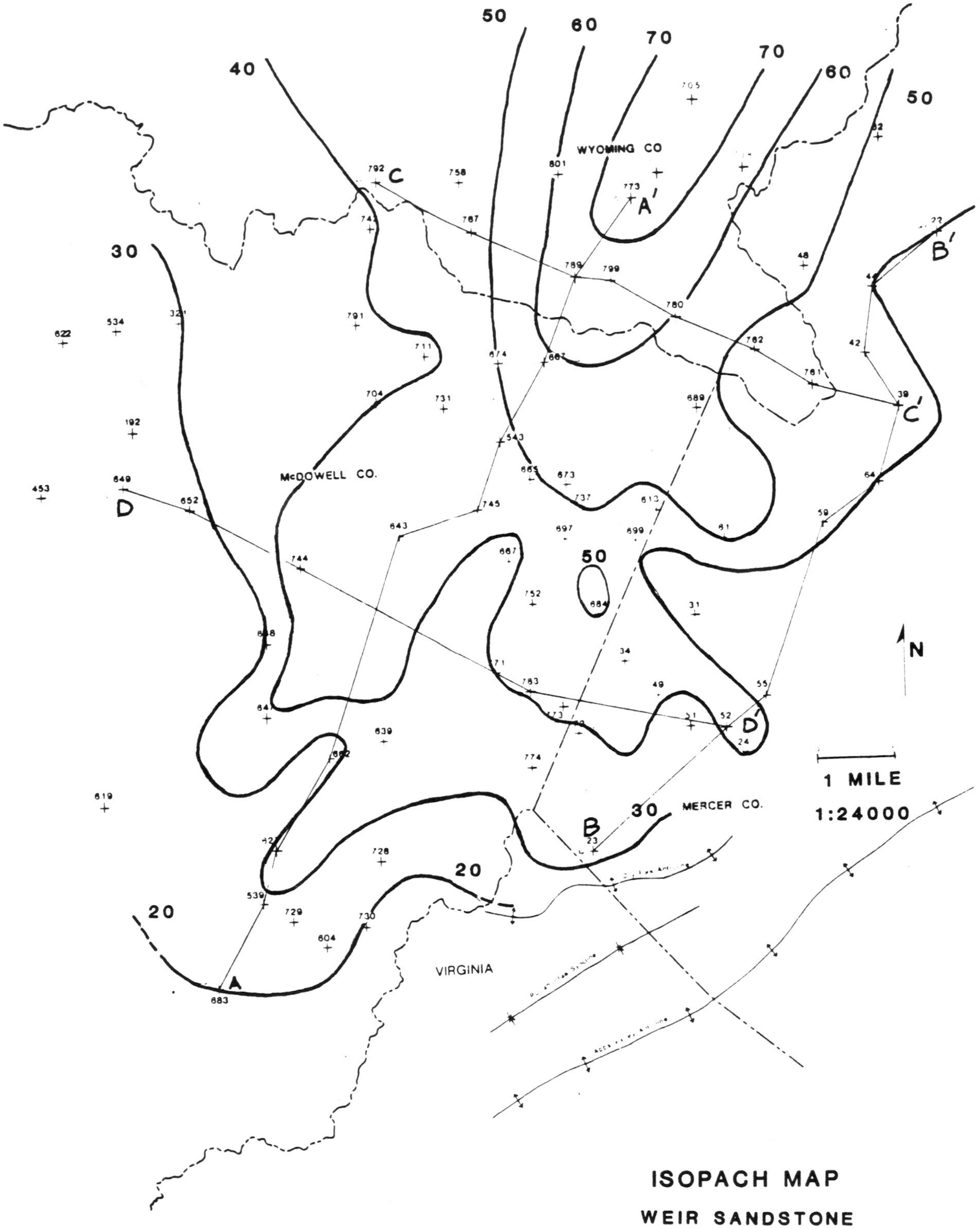

ISOPACH MAP

WEIR SANDSTONE

CONTOUR INTERVAL 10 ft.

Figure 8

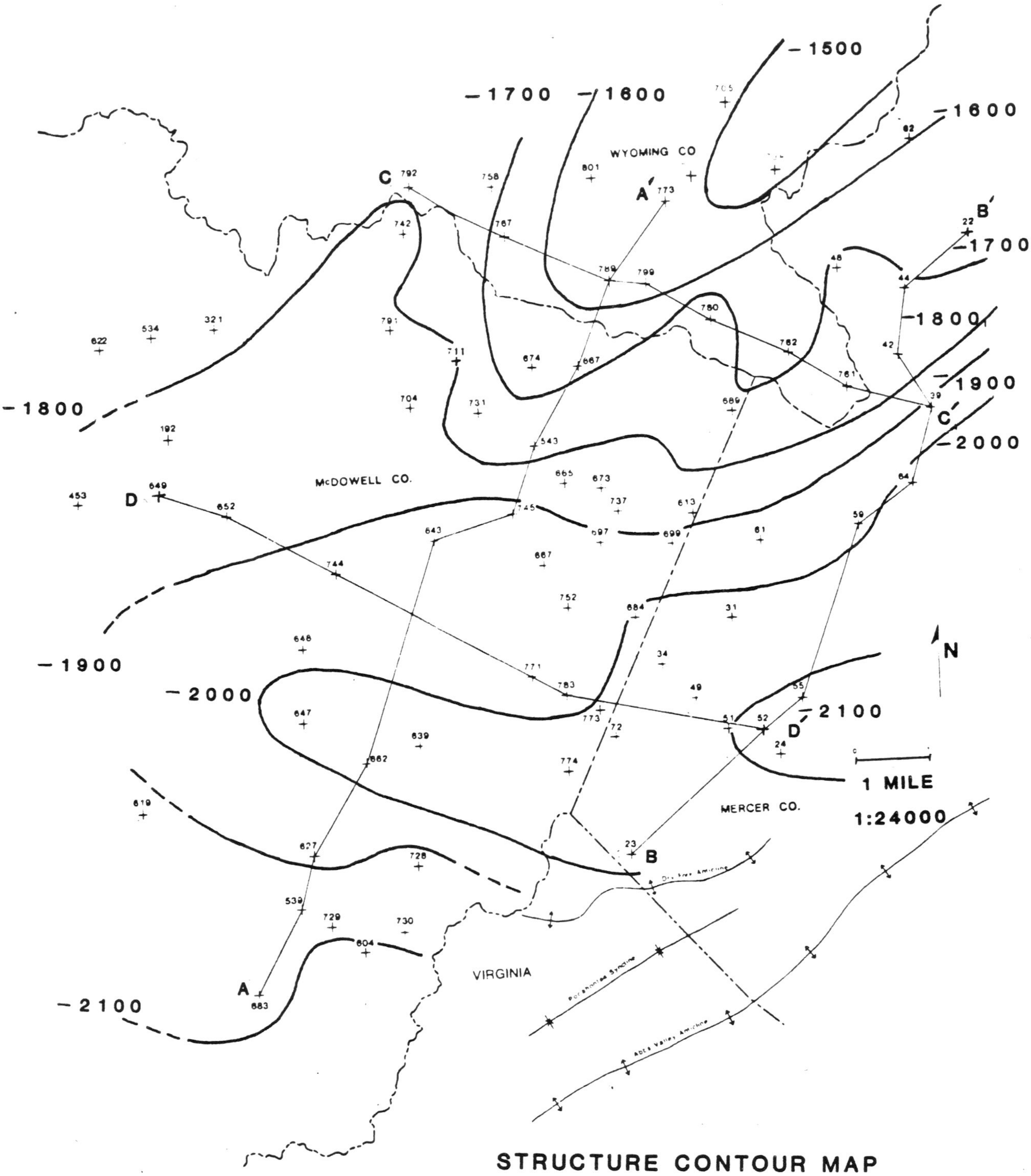

STRUCTURE CONTOUR MAP
WEIR SANDSTONE

Figure 9 DEPTH BELOW SEA LEVEL IN FEET
CONTOUR INTERVAL 100 ft.

cross section D-D', shows the Weir thinning to the northwest. These seemingly anomalous trends can be understood when viewed within the broader regional context shown on the isopach map (Figure 8). The Weir appears to be a prograding distributary-mouth-bar with a northern source. This interpretation is consistent with the depositional environment postulated for the Weir by Bartlett (1974) and Williamson (1974). Production trends within the field are controlled by unit thickness and by surrounding structural features. The structural features that bound the field to the east, the Dry Fork and Abbs Valley anticlines, limit production on the east side, while thinning of the Weir limits production to the south and west. The structure contour map (Fig. 9) shows a synclinal structure in the southern part of the field but it has no apparent effect on production. A plunging anticlinal feature in the northern part of the field generally correlates with increasing unit thickness on the isopach map. Present expansion of the field is along the trend of this anticline. The 30-foot isopach generally defines the limits of production throughout most of the field with only a few wells producing from the Weir where it is less than 30 feet thick. Attempts to relate gas production to thickness were unsuccessful due to a lack of data on initial flow rates and variations in physical treatments used to enhance production.

Previous Investigations

The Pocono Group was first described by Rogers (1838) and was further detailed in his later reports. Rogers designated the Paleozoic formations of the Appalachian region by a series of Roman numerals under which the Pocono was labeled Formation X. Later, he renamed the formations using a series of Latin names, and Formation X became the Vespertine Formation. Campbell (1894) assigned the name Price Formation to the southern portion of the unit due to an exposure on Price Mountain in Montgomery County, Virginia. The northern and western outcrops had previously been named the Pocono Sandstone in West Virginia and Pennsylvania by Ashburner (1876), resulting in two names for what is essentially the same stratigraphic unit. The dividing line between the two "formations" varies among authors; some use the New River and others the James River. Use of the two names would be justified if the dividing line corresponded to a facies change, but the boundary is purely geographic. Butts (1940) recognized that the Price and Pocono Formations were stratigraphically equivalent, and he recommended that the formation be named the Price-Pocono Formation since both names were so well entrenched in the literature.

Most later stratigraphic studies were concentrated in the outcrops in southeastern West Virginia and southwestern Virginia. Fontaine (1877), Campbell (1894), and Stevenson (1903) described stratigraphic sections and Branson (1912) first interpreted the Pocono as a deltaic sequence.

Reger (1926), in his county report for Mercer, Monroe, and Summers Counties, subdivided the Pocono into various members. Among Reger's members was the Broadford Sandstone, which he named after the town nearest its type area in Tazewell County, Virginia. He correlated the Broadford Sandstone to the Weir oil sand of Kanawha County, West Virginia. Woodward (1932) and Chadwick (1935) described stratigraphic sections and Cooper (1937), Butts (1940), and Glover (1953) postulated depositional environments for portions of the Pocono. Larger scale regional studies include those of Pepper _et al._ (1954) who studied the depositional environment of the Pocono in parts of West Virginia and Ohio, and Pelletier (1958) who studied depositional environments in West Virginia and Pennsylvania. Dally (1956) studied the paleontology and stratigraphy of the Pocono in West Virginia.

Previous petrographic studies that have included stratigraphic equivalents of the Weir have been broad, regional studies. Since the Pocono is known for lithologic variability, these studies have limited geographic applicability. Walker (1964) gave detailed petrographic descriptions of the Price Formation in southwestern Virginia. Heald (1965), in his study on lithification of sandstones in West Virginia, gave descriptions of Mississippian sandstones but did not differentiate the Weir from others. Kerisa (1972), in his provenance study of the Price Formation in Virginia, gave detailed petrographic descriptions of units equivalent to the Weir. Bartlett (1974) and Williamson (1974) studied the depositional environments of the Pocono and Price Formations in eastern West Virginia and southwestern Virginia, and southern West Virginia, respectively.

Methods

Modal Analysis

Modal analysis of constituents was performed using the point count method of Chayes (1956). Twelve parameters were measured by point counting 300 points per thin section. A chart published by van der Plas and Tobi (1965) shows the reliability of point count data in achieving statistically valid results. Estimates of abundance for any given constituent based on 300 points per thin section have a maximum error of ± 5% for constituents comprising greater than 25% of the sample, ± 4% for these comprising 5% to 25% of the sample, and within less than ± 3% for samples comprising less than 5% of the sample (at a 95% confidence level).

Grain Size Measurement

Average grain size was calculated by measuring the apparent long axis of quartz grains with an ocular micrometer. Three successive measurements of 25 grains each within a single thin section produced a mean size within ± 0.01 mm of the mean for 3 measurements in separate thin sections. It was concluded that 75 measurements of grain size per thin section would give accurate results, bcause the unit is so homogeneous.

Thin Sections

Samples for thin sections were cut parallel to core length and taken from core centers to reduce the degree of contamination from drilling fluids. Samples were taken at uniform intervals through thick units and at any obvious lithologic changes. Thirty-three thin sections were prepared by Roberts Petrographic Service, and 23 of these were impregnated with a blue epoxy following the procedure of Gardner (1980). The impregnation procedure, which uses a low viscosity epoxy, low pressure, and a long curing time, serves 3 purposes: 1) to aid in porosity studies by using easily identifiable epoxy; 2) to provide samples for pore cast studies; and 3) to preserve the authigenic clay minerals which may be removed during normal thin section processing (Carrigy and Mellon, 1964). Additional thin sections included 0.20 mm thick thin sections for use in luminescence studies as suggested by Furbish (1974).

Staining

Thin sections were stained to aid in the identification of feldspars (Boone and Wheeler, 1968). Their method consists of the following steps: etching the uncovered thin section for 15 seconds in vapors of 52% hydrofluoric acid (HF), immersion in a solution of sodium cobaltinitrite, immersion in a solution of barium chloride, immersion in a solution of amaranth red stain, and covering. Thin sections are rinsed and air dried between each step. This procedure stains potassium feldspars yellow and plagioclase feldspars red. Clay minerals, matrix and calcite may be stained slightly red but not enough to interfere with identification of the feldspars.

Pore Casts

Pore casts were used to study the pore geometry in selected samples. They were prepared by dissolving the lithic material from samples that had been impregnated with epoxy (Pittman and Duschatko, 1970). The technique involves 2 acid treatments that do not dissolve the epoxy. First, the carbonate minerals were dissolved using dilute hydrochloric acid (HCl). The carbonate minerals must be removed first because they will react with the HF, used in the following step, to form insoluble calcium fluoride (Grayson, 1956). Silicate minerals were then removed using HF. Samples were immersed in a 52% HF solution for 72 hours. The HF was replaced and the samples were agitated in an ultrasonic bath after 24 hours to remove insoluble residue and to ensure complete dissolution of the silicate minerals. After the samples were carefully washed and dried, they were mounted and coated for examination using the scanning electron microscope (SEM).

Scanning Electron Microscope

An ISI-40 scanning electron microscope was used to study the texture, mineralogy, and pore geometry of selected samples. The primary use of the SEM was to identify authigenic minerals by their crystal morphology, provide 3-dimensional images of pore spaces, and to study the relationship of authigenic minerals to pore spaces. Samples examined included chips from core samples, thin sections, and epoxy pore casts.

X-Ray Diffraction

X-ray diffraction aided mineralogical analyses of whole rock samples and the clay size fraction. Analysis of the whole rock samples utilized uncovered thin sections. Separation of the clays (4 microns) was accomplished using settling techniques described by Folk (1974). The clay fraction was concentrated by crushing rock chips taken from the center of cores. Due to the scarcity of clay minerals in the samples, 75 milliliter (ml) samples of a clay-water suspension were taken to ensure samples of useable size. The samples were evaporated at 75°C until approximately 10 ml of solution remained. This slurry was placed on 3 slides and was allowed to settle and dry in order to enhance the basal reflections of the clays. One slide was analyzed before and after heating for 2 hours to 600°C to differentiate kaolinite from chlorite (Thorez, 1976). The second slide was analyzed for expandable layer clays by exposure to an atmosphere saturated with ethylene glycol for a minimum of 2 hours at 60°C. The third sample was kept as a reserve. Diffractograms were obtained using a GE-700 Diffractometer with nickel filtered copper (K-Alpha) radiation using standard x-ray techniques.

Semi-quantitative analysis of the clays was based on the method used by Thorez (1976). This method gives an approximation of the relative abundance of clay minerals based on the heights of the basal reflections (the 001 peaks) measured above the level of background radiation for glycolated samples. Preliminary studies of the clays indicated a lack of expandable layer clays, so glycolating samples was unnecessary. Thorez used the full height of all clay mineral 001 peaks with the exception of kaolinite. The peak height of kaolinite must be divided by a factor of 2 for poorly crystallized kaolinite or a factor of 3 for well crytallized kaolinite. Because the crystallinity of the kaolinite in the samples was not known, a value of 2.5 was used as an estimate. Division by this factor is based on the assertion by Weaver (1958) that the 001 peak of kaolinite is 2 to 3 times more intense than the 001 illite peak due to the distribution of diffraction intensities. The measured heights of all 001 clay peaks were summed and divided into 10. The resulting factor was multiplied by the individual peak heights for each clay mineral to provide an estimate of its abundance relative to other clay minerals in the sample. The sum of all values for any given sample will be 10. These estimates were used to describe relationships between clay minerals and porosity and they are meaningful only when compared among samples within this study.

PETROLOGY

Core Analysis

Two 4 inch diameter cores, each with approximately 25 feet of Weir sandstone, were available for this study. The cores were supplied by Consolidated Gas Supply Corporation from C.G.S. wells 11495 and 11498; West Virginia Geological and Economic Survey county permit numbers McD 539 and 543, respectively. The Weir is primarily massive, fine-grained, gray sandstone with basal shales (Fig. 10).

Neither of the two cores represent an entire section of the Weir, nor are they stratigraphically equivalent. Core McD 543 represents approximately the lower half of the Weir. McD 539 is from the central portion of the Weir, with only its uppermost and lowermost portions not cored. Hence, the cores overlap stratigraphically and the upper part of McD 543 is partially equivalent to the cored section in McD 539. Initial examination of samples in proximity to intercalated shales in McD 543 and to the basal shale in McD 539 show they differ, in both porosity and mineralogy, from the upper massive sand. The differences are directly related to the presence of the shales. In order not to give a distorted impression of the characteristic massive Weir sand, it is divided into an upper and lower portion based on porosity. The upper portion is defined as the interval with porosity greater than or equal to 10% and the lower portion as the interval with less than 10% porosity (Figure 10). Subsequent references to the upper and lower Weir refer to this porosity-based subdivision.

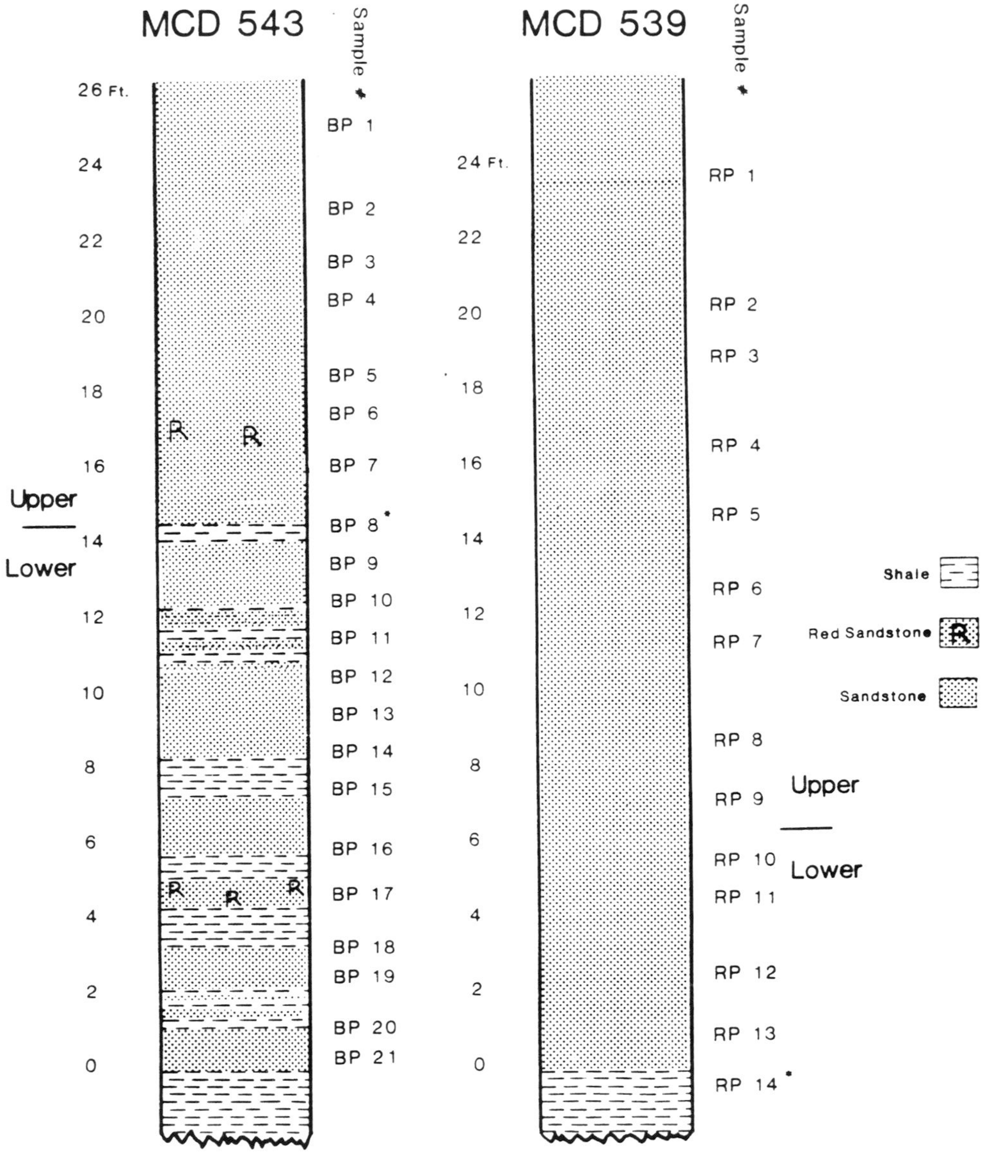

Figure 10. Lithologic description of cores MCD 543 and 539. Sample numbers show the location of thin sections. "Upper" and "Lower" designate the division of the Weir based on porosity. The two cores are not stratigraphically equivalent. * Denotes samples with out thin sections.

Contacts between the sand and shale are generally sharp except where loading has disrupted thinly bedded units. Sedimentary structures consist primarily of load structures, including small (2 to 3 cm) ball structures, load piled ripple marks, and convoluted bedding. Traces of ripple marks are found at several sand-shale contacts but the ripples are small, less than 1 cm amplitude, and poorly preserved.

Fossils are rare in the samples; only a few small bivalves and plant fragments were found. The bivalves occur primarily in one sample, BP 9, 2 cm below a sharp sand-shale contact. They are disarticulated, randomly oriented, and average about 5 mm in length. The plant fossils are less tha 1 cm in length and found only in shale laminae.

Several zones of reddish-brown sand occur in sharp contact with the more usual gray sand. Color changes are not related to lithologic variations, and thin section studies show that the red coloration is due to oxidation of iron in authigenic siderite to form limonite.

Sandstone Classification

The mean percentages of quartz, feldspar, and rock fragments, when recalculated to 100%, are 72%, 5%, and 22%, respectively. These percentages, when plotted on the ternary diagram of Folk's (1968) sandstone classification, reveal that the Weir sand is a lithic arenite (Fig. 11). More specifically, the Weir is a sedarenite because the percentage of sedimentary rock fragments (SRFs) is approximately three times greater than the percentage of metamorphic rock fragments (MRFs). The petrographic uniformity of the Weir can be shown by plotting samples with the recalculated minimum and maximum values of the end members on the ternary diagram. All points plotted for these samples lie within the boundaries of lithic arenites.

The Weir is almost identical to the genetic subtype of lithic arenite which Folk classifies as a miogeosynclinal phyllarenite (Folk, 1974), the only petrographic difference being the lower percentage of MRFs in the Weir. Folk suggests that these types of sediments were produced by "... horizontal deformation on a protocontinental margin causing uplift and converting the sediments to their low-grade metamorphic equivalents." This explanation agrees with the general tectonic history postulated for the study area during the Early Mississippian (Briggs, 1974).

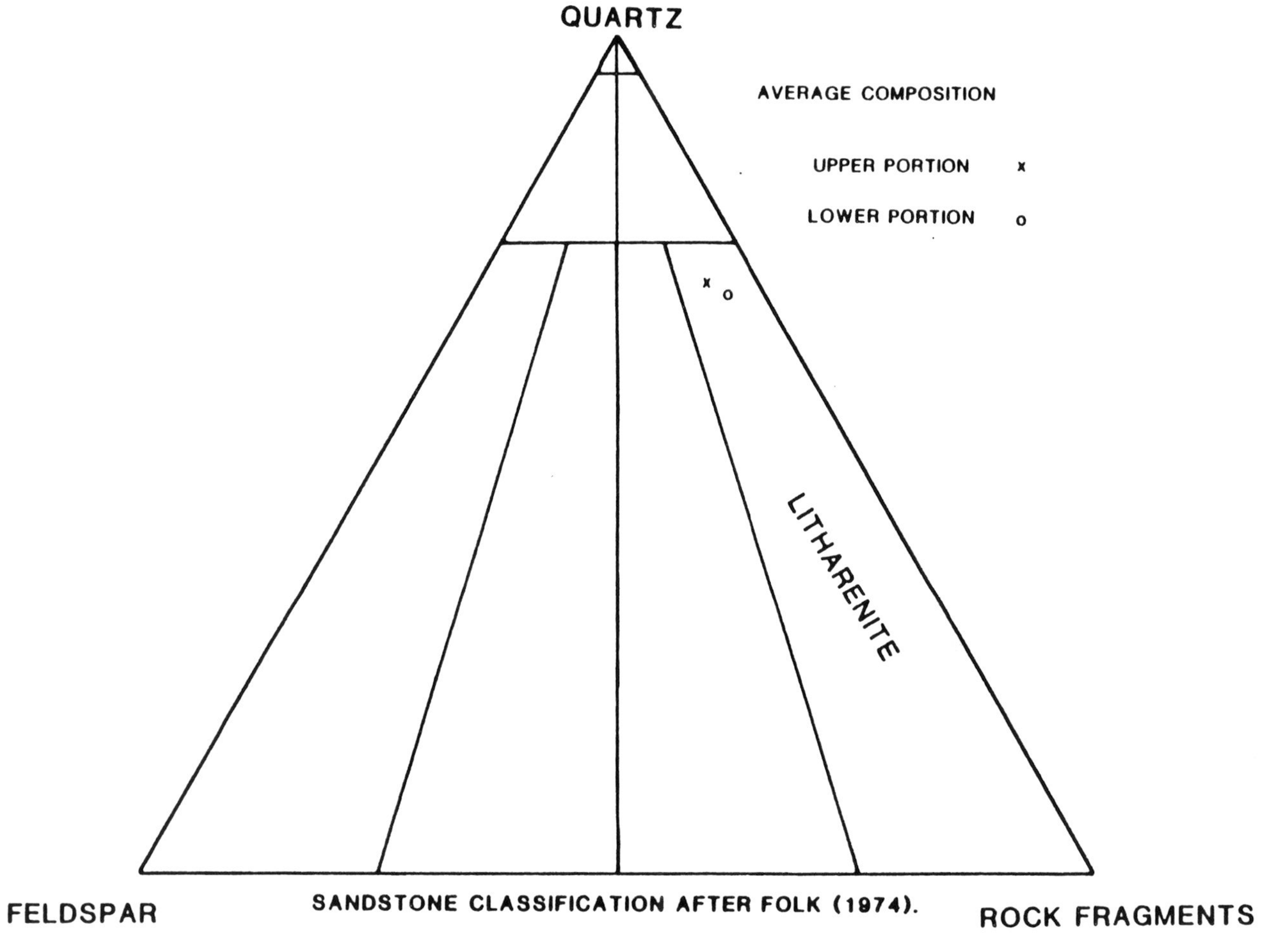

Figure 11. Sandstone classification.

Detrital Constituents

Quartz

Detrital quartz is the primary constituent of the Weir sand, averaging 54% (S.D. ± 4%) and ranging from 40% to 59% (Fig.12). Grain size ranges from 0.003 mm to 0.34 mm with a mean diameter of 0.107 mm (Fig. 13). Grain shape varies from equant to elongate and roundness varies from subrounded to angular. Quartz grains are dominantly (96%) monocrystalline. A small percentage of polycrystalline grains in the fine to very fine sand size range is to be expected due to the mechanical breakage of coarse polycrystalline grains during sedimentary transport (Boggs, 1968). The quartz grains are clear to slightly turbid and commonly have inclusions. Most inclusions are small fluid filled vacuoles. Some grains have dark, subparallel lines of small vacuoles. These lines are known as Boehm lamellae (Scholle, 1979) and they form due to strain produced by overburden pressure. Rod-shaped rutile is the most common type of inclusion; but inclusions of all types are found in only 5% of the quartz grains.

Rock Fragments

Rock fragments comprise an average of 17% of the Weir, with a range of 10% to 23%. MRFs average approximately 5% and SRFs average approximately 12%. The MRFs consist of slate, phyllite, schist, and quartzite fragments. Slate, phyllite, and schist fragments are differentiated from the SRFs by the large size and parallel orientation of the mica in

WEIR COMPOSITION
(Mean %)

	UPPER PORTION	LOWER PORTION	COMBINED
QUARTZ	55	53	54
ROCK FRAGMENTS	18	17	17
FELDSPAR	5	4	5
CARBONATES	4	12	9
MATRIX	4	7	5
POROSITY	11	4	7
OTHER	3	3	3

Figure 12. Average composition for the upper, lower, and combined Weir samples. "Others" includes accessory minerals, sulfates, and pyrite. Porosity is Core Lab. porosity.

Sample Number	Dia.(mm)
RP 1	0.114
RP 2	0.119
RP 3	0.129
RP 4	0.122
RP 5	0.104
RP 6	0.096
RP 7	0.101
RP 8	0.124
RP 9	0.123
RP 10	0.106
RP 11	0.130
RP 12	0.135
RP 13	0.111

Mean Dia. 0.116

Sample number	Dia. (mm)
BP 1	0.157
BP 2	0.130
BP 3	0.118
BP 4	0.121
BP 5	0.120
BP 6	0.102
BP 7	0.124
BP 8	shale
BP 9	0.107
BP 10	0.096
BP 11	0.104
BP 12	0.096
BP 13	0.107
BP 14	0.099
BP 15	0.103
BP 16	0.111
BP 17	0.088
BP 18	0.098
BP 20	0.092
BP 21	shale

Mean Dia. 0.108

Figure 13. Mean grain size of quartz grains from point counts. Diameter measured along the long axis in millimeters.

the fragment, and quartzite is distinguished by its polycrystalline grains with sutured contacts between the subgrains and by common inclusions of muscovite along the subgrain contacts. The slate fragments are characterized by the parallel orientation of the clays; the phyllite and schist fragments, by the abundance of well oriented muscovite. Rare fragments of chlorite schist are distinguished by their characteristic green color.

SRFs consist of shale fragments and minor amounts of siltstone and chert. The shale fragments are illitic in composition and they lack the orientation of the clays exhibited by slate. Gradational fragments do exists, and reliably identifying such grains is difficult. The siltstone fragments are recognized on the basis of silt-size quartz and the cherts are characterized by a black and white speckled pattern. The deformation of low-grade MRFs and shale fragments creates a 'pseudomatrix' which is often difficult to distinguish from true matrix material. The percentage of rock fragments is greater in this study than in previous reports; the percentage of matrix is correspondingly lower. This is due to the high magnification (up to 630X) used during point counting which allowed greater discrimination between deformed rock fragments and matrix material.

Feldspars

Feldspars average approximately 4% of the Weir with a range of 3% to 8%. The mean grain size is approximately 0.09 mm and the grains are generally subangular and equant in shape. The feldspars are predominantly plagioclase. The plagioclase is sodium rich, with a compositional range from approximately An 10 to An 50 as determined by extinction angles. Clear, slightly to moderately altered, untwinned albite is the most common feldspar. Twinned plagioclase has a wide range of composition from albite to andesine. The twins are primarily albite twins, with rare Carlsbad and perthitic twins. The degree of alteration varies from negligible to almost complete replacement. It is commonly altered by sericitization which gives the grain a turbid appearance in plane light.

Rare grains of potassium-feldspar (K-feldspar) are the same size and shape as the plagioclase grains but they have spindle twinning. These grains represent fragments of microcline (Scholle, 1979). The inability to recognize both grid twinning and Carlsbad twins is due to the small size of the grains. Larger feldspar grains would be preferentially broken along cleavage planes during transport and would contribute untwinned fragments of the original grain to the smaller size fraction (van der Plas, 1975). The abundance of K-feldspar may be underestimated due to the size and extreme alteration of the grains, which often make positive identification impossible.

Accessory Minerals

Accessory minerals found in the Weir consist of muscovite, pyrite, amphibole, rutile, biotite, zircon, hematite, and ilmenite. The two most common accessory minerals are pyrite and muscovite. Pyrite averages 1% of the rock with a range of 0 to 4%. It is found as pore filling masses of euhedral crystals. Muscovite occurs as elongate detrital grains and averages 1% of the rock with a range of 0 to 2%. The remaining accessory minerals all average less than 1%. Amphibole, in the form of hornblende, is moderately altered and occurs as subrounded, equant grains. Rutile is rare in the Weir but is easily recognized by its brown color, high relief, and elongate shape. Biotite is found as elongated flakes with a greenish-brown color. The greenish color suggests that the biotite is being altered to chlorite. Zircon is easily recognized by its very high relief and high birefringence. Hematite is found as very small, euhedral crystals in pore spaces and as a reddish stain. Ilmenite and possibly magnetite are found in small, opaque crystal masses. Both are bluish-black in reflected light and it is difficult to differentiate between them. The ilmenite often appears to be altered to leucoxene, which occurs as a white, resinous coating on the ilmenite.

Matrix Material

Matrix material is defined in this study as material less than 0.03 mm in diameter and without distinctive shape. Lack of distinctive shape is included in the definition in order to exclude material created by the deformation of ductile rock fragments. Examination of the samples at high magnification revealed only 5% matrix. This material is primarily fine silt-size quartz, accessory minerals, and clays. The mineralogy of the clays is difficult to determine but they appear to be primarily illite. The origin of the matrix is impossible to determine. Much of the material is probably from rock fragments and some of the clay is probably authigenic in origin.

Interpretation

The presence of both MRFs and SRFs suggests a dual source area for the Weir. The MRFs and elongate, angular, composite quartz grains indicate a significant contribution of sediments from a metamorphic terraine. The presence of chlorite schist, clear untwinned albite, and the lack of other metamorphic minerals indicates the terraine has been subjected to conditions characteristic of greenschist facies metamorphism (Miyashiro, 1973). The abundance of SRFs shows that a major portion of the sediments has been derived from a sedimentary source. The rounded quartz grains are probably reworked from sandstone and the shale clasts may be from reworked pelitic deltaic material. The abundance of shale clasts indicates that the sediments have undergone only brief transport (Folk, 1974). There is also a possibility that an igneous source has contributed to the Weir. Walker (1964) described igneous rock frgaments (IRFs) to the east of the study area from a conglomerate that is stratigraphically equivalent to the Weir. The lack of IRFs in the study area could be due to breakage, with characteristically coarse particles being broken into component minerals not recognizable as IRFs (Boggs, 1968). However, the small amount of K-feldspar suggests only a minor contribution by the igneous rocks.

Authigenic Minerals

Chlorite

Chlorite is the most abundant authigenic mineral in the Weir. It occurs as discrete crystals approximately 0.007 mm in length. The crystals are oriented normal to the detrital grain surfaces on which they form a thick grain coating. The chlorite is green in plane light, has moderate birefringence in polarized light and is most abundant in the upper portion of the Weir.

Illite

Illite occurs as irregular grain coatings in the form of small, fibrous crystals oriented parallel to detrital grain surfaces. The illite is easily distinguished from chlorite by its higher birefringence and by the orientation of its crystals. Authigenic illite is not quantitatively important in the Weir. Although major illite peaks are found on XRD patterns, most of the illite can be attributed to detrital sources.

Kaolinite

Kaolinite occurs as rare, well defined crystals filling pore spaces and as *in situ* replacement of K-feldspar, which is the dominant source of this mineral. Replaced feldspar grains retain their original shape but appear brown in plane light and white in reflected light. The kaolinite has low birefringence and is found in greatest abundance in the upper portion of the Weir.

Sulfates

Anhydrite and barite are found in minor quantities as pore fillings in the lower portion of the Weir. Anhydrite is recognized by its high birefringence, second and third order red and green colors, and 90 degree cleavage. Barite is characterized by its low birefringence, high relief, and 90 degree cleavage. Anhydrite averages less than 1% of the total sediment and ranges from 0 to 4%. Barite consistently comprises less than 1% of the rock. Both occur as pore fillings, apparently replacing carbonates, and are found in close association with the interbedded shales.

Carbonates

Carbonates found in the Weir consist of calcite, siderite, and dolomite. Calcite occurs as pore fillings in large (0.3 mm), subhedral masses commonly with poikilotopic texture. In the lower portion of the unit, it often occurs as smaller crystals mixed with siderite to form a carbonate matrix. Siderite occurs as small (0.02 mm) crystals with a flattened rhombohedral shape. It is abundant in close proximity to interbedded shales and often has a brownish coating of limonite. Siderite can be distinguished from calcite and dolomite by the flattened shape of the crystals and by the brownish color. Dolomite occurs as rare, euhedral rhombs which are larger than the siderite crystals. It is found in the lower portion of the Weir in samples with large amounts of siderite.

Secondary Quartz

Quartz overgrowths are found throughout the Weir as both syntaxial and polygonal overgrowths. These overgrowths comprise approximately 2% of the total quartz and act as a cement. The syntaxial overgrowths are identified by dust rims which separate the optically continuous overgrowth from the detrital grain. Quartz overgrowths forming a "polygonal grid" texture were found where authigenic clay, primarily illite, form irregular coatings on detrital grains. The overgrowths nucleate in gaps within the clay coatings and incorporate the clay into the overgrowth (Heald and Larese, 1974). The polygonal overgrowths are easily recognized by the high birefringence of the illite crystals which are oriented normal to the surface of the detrital grain.

X-Ray Diffraction

X-ray diffraction (XRD) was used to confirm the presence of minerals previously identified petrographically, and to provide information on the mineralogy, crystallinity, and abundance of clay minerals. Both whole rock samples and the less than 4 micron (clay) fraction were analyzed using a variety of chemical and physical treatments to aid in the identification of specific minerals.

XRD patterns of whole rock samples primarily show minerals that comprise at least 5% of the total sample. The presence of quartz, plagioclase, calcite, and siderite are clearly shown, but only traces of clay minerals are evident. XRD patterns for clay minerals and accessory minerals are of low intensity and poorly defined, and do not allow for positive identification due to the low concentration of the minerals. For this reason, the clay fraction was separated and analyzed.

The less than 4 micron (8 0) fraction consists of quartz, illite, chlorite, kaolinite, and siderite. The quartz and siderite occur in this fraction due to the mechanical processing of the samples. Quartz is found in all samples while siderite occur only in samples from the lower portion of the unit.

Illite is the most common clay mineral in the Weir because it occurs both as an authigenic grain coating and as a major constituent in shale clasts. XRD patterns show a high ratio of 10 Angstrom (A) to 5 A peak intensities, which suggests a dioctahedral crystal structure (Thorez, 1976) and a high iron content (Grim, _et_ _al_, 1951). The shape of the

10 A peak, prior to heat treatment at 600°C, suggests the illite is moderately to well crystallized. The increase in intensity of the 10 A peak after heat treatment also suggests a dioctahedral crystal structure (Thorez, 1976). The 10 A (001) peak is slightly asymmetric to the right, which suggests the presence of minor quantities of mixed-layer, illite-semectite clays (Fig. 14).

Chlorite is found throughout the Weir and varies in both crystallinity and abundance. Chlorite is identified by its basal (001) peak at 14.1 A, and by the (003) peak at 4.72 A. It is a trioctahedral variety as shown by the (006) peak at 1.53-1.54 A, and is iron rich as shown by the broader and more diffuse (001) peak after heat treatment at 600°C (Carroll, 1970). The chlorite shows no change upon glycolation. Heat treatment suggests it is well crystallized since poorly crystallized chlorite would decompose at temperatures greater than 450°C (Thorez, 1976).

The presence of kaolinite is indicated by peaks at 7.15 A (001) and 3.57 A (002). The peaks are sharp and well defined which indicates well crystallized, authigenic kaolinite. The presence of chlorite complicates the identification of kaolinite because the (001) and (003) chlorite peaks occur at 7.15 A and 3.56 A, respectively, which masks the (001) and (002) kaolinite peaks. This problem was solved by using two methods to distinguish chlorite from kaolinite. First, heat treatment at 600°C for one hour collapses the kaolinite peaks but has little effect on the chlorite. Secondly, the chlorite was removed by treating the sample with warm HCl acid. This acid treatment has no effect on kaolinite.

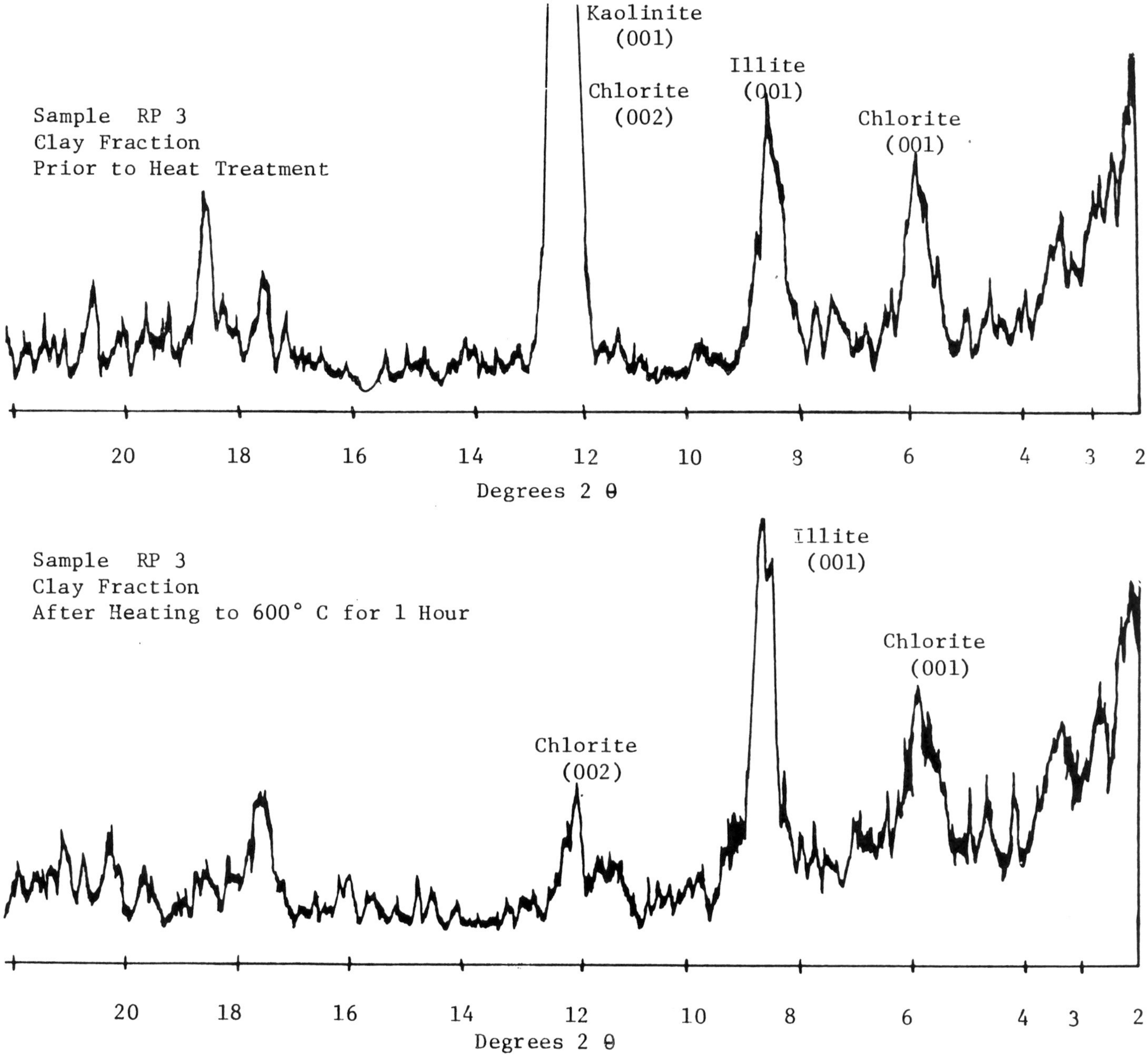

Figure 14. Sample RP 3 showing the effect of heat treatment. Note the collapse of the kaolinite peak, and the increased intensity of the illite peak.

Interpretation

Figures 15 and 16 graphically show the relationship of the estimated abundance and distribution of clay minerals to porosity. The charts were constructed using semi-quantitative estimates of clay abundance and Core Lab porosity estimates. Increased kaolinite and chlorite abundance correlates with increasing porosity. Illite decreases in abundance with increasing porosity. The sharp illite peaks in the figures correspond to the illite-rich nature of the interbedded shales. The small amount of chlorite shown in the figures is due to two factors: 1) the chlorite is iron-rich, which produces a low intensity peak that suggests lower chlorite values relative to the other clays; 2) the chlorite is the only clay that formed primarily from solution. Only a small portion of illite or kaolinite formed from solution. They were formed primarily from the *in situ* alteration of detrital material and hence are found in abundance throughout the Weir. The greater abundance of kaolinite in higher porosity samples is due to the increased availability of interstitial fluids for the alteration of K-feldspars to kaolinite.

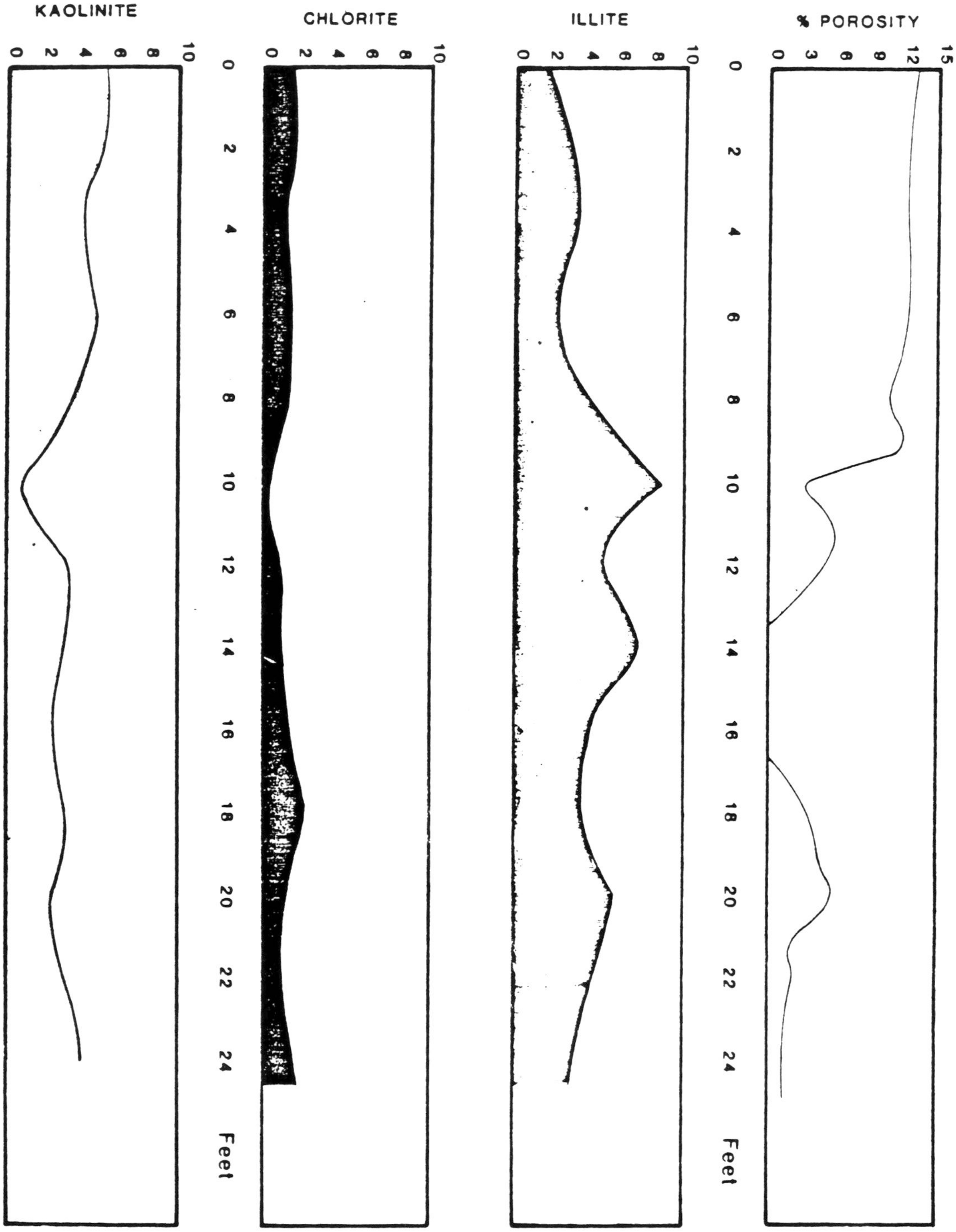

Figure 15. Porosity vs. Clay Abundance, MCD 543. Estimates of clay abundance are based on the method of Thorez (1976). Values of clay abundance are in unitless numbers.

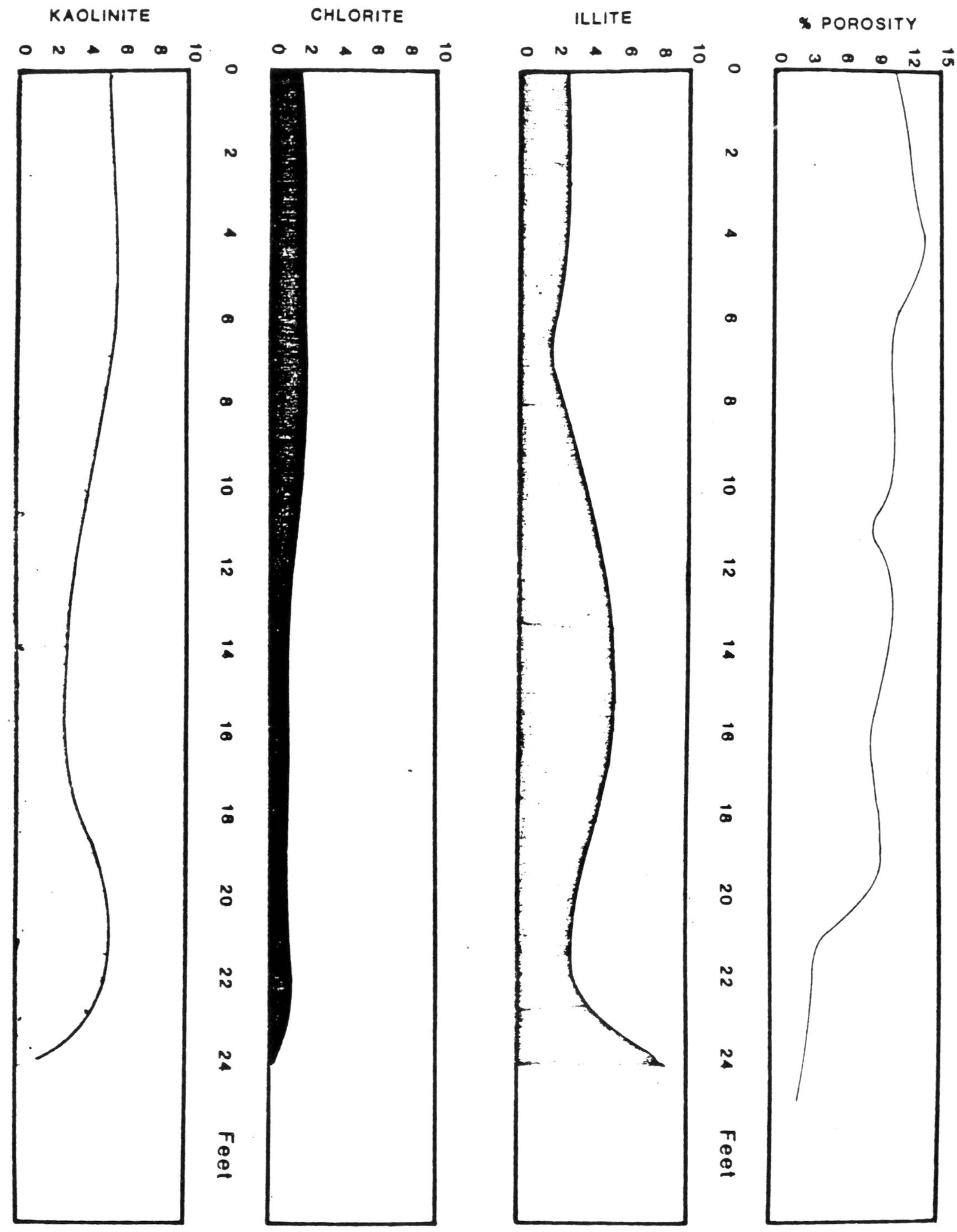

Figure 16. Porosity vs. Clay Abundance, MCD 539. Estimates of clay abundance are based on the method of Thorez (1976). Values of clay abundance are in unitless numbers.

POROSITY

Introduction

Pore space in the Weir consists of both primary and secondary porosity. Primary porosity is the pore space formed during deposition of the sediments, while secondary porosity is pore space created by diagenetic processes after deposition. Primary porosity is usually only a fraction of the original porosity due to subsequent changes by mechanical compaction. Secondary porosity is more complex in nature than primary porosity because it can form by several processes. Schmidt and McDonald (1979) recognized 5 genetic classes of secondary porosity based on processes of origin and textural relationships. These 5 classes are porosity created by: (1) fracturing, (2) shrinkage, (3) dissolution of detrital grains, (4) dissolution of authigenic cementing materials, and (5) dissolution of authigenic replacement minerals. Fracture and shrinkage porosity generally have characteristic patterns which are recognizable. Dissolution porosities, however, are often difficult to distinguish from primary porosity and are often misidentified. The textural classification used in this study is based on the nomenclature of Choquette and Pray (1970), which includes the terms intergranular, intragranular, and reduced porosity. In addition, the term "microporosity," as defined by Pittman (1979), is used for pore space less than 0.05 microns in diameter. This term is used primarily to describe pore space between clay crystals.

Porosity Distribution

The average porosity of the Weir is 7%, with a range from 0 to 13.2% as measured by mercury injection tests performed by Core Laboratories, Inc. The upper portion averages 10.7% with a range from 10% to 13.2% and the lower portion averages 4% with a range of 0 to 9.6%. Point count data generally correspond well with results of the injection test. The combined point count porosity averages 7.6% and the upper and lower portions average 10.9% and 4.4%, respectively. Permeability values are low; the average permeability for the upper portion is less than 0.2 millidarcys (md) and ranges from less than 0.1 md to 0.8 md and consistently less than 0.1 md for the lower portion.

Primary Porosity

Approximately 90% of the total porosity and greater than 95% of the effective porosity is primary. Total porosity is the sum of all pore space and effective porosity is the sum of all interconnected pore space. Porosity in the Weir is intergranular, reduced primary porosity. The pore space is created by a framework of detrital grains and is reduced in volume by pore linings of authigenic chlorite (Fig. 17).

Secondary Porosity

Secondary porosity in the Weir accounts for approximately 10% of the total porosity and less than 5% of the effective porosity. The secondary porosity was created by: (1) dissolution of detrital grains;

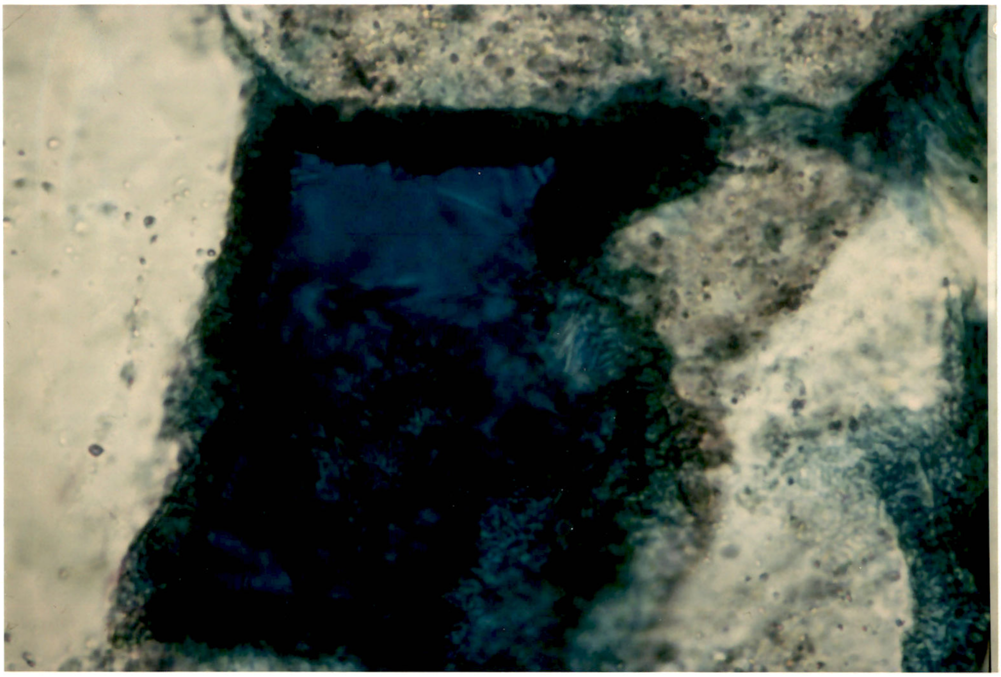

Figure 17. Sample from the upper portion of the Weir showing reduced intergranular primary porosity. Blue material is colored epoxy filling pores. Dark material lining the pores is authigenic chlorite. (250x)

(2) dissolution of authigenic cementing mineral, and (3) microporosity. Dissolution of detrital grains is most important. Rock fragments and feldspars commonly show evidence of post-depositional dissolution. Evidence for the inplace dissolution of the grains is shown by the fragile condition of what remains of these grains (Figure 18). These detrital grains could not have survived sedimentary transport in their present fragile condition. Approximately 5% of the rock fragments and 10% of the feldspars show evidence of dissolution. The total volume of pore space formed by dissolution of detrital grains is minor and the increase in effective porosity is small. The second type of secondary porosity is created by the dissolution of authigenic minerals. Authigenic calcite appears to have undergone partial dissolution in a small percentage of calcite pore fillings found in the Weir, as evidenced by the rounded edges and the pore space around the calcite grains. These rounded grains represent an early calcite pore filling that was partially dissolved. The amount of early calcite that underwent dissolution is indeterminable; therefore, the amount of secondary porosity created is impossible to estimate. If significant amounts of calcite were dissolved, then the percentage of secondary porosity estimated by this study would have to be increased. The third type of secondary porosity found in the Weir is microporosity. Microporosity is created by the dehydration of clay or mud clasts. The water is driven off during diagenesis but the clasts retain their original size. The pore space occupied by the water becomes intraparticle microporosity (Fig. 19). Evidence for this type of porosity is that colored epoxy penetrates the

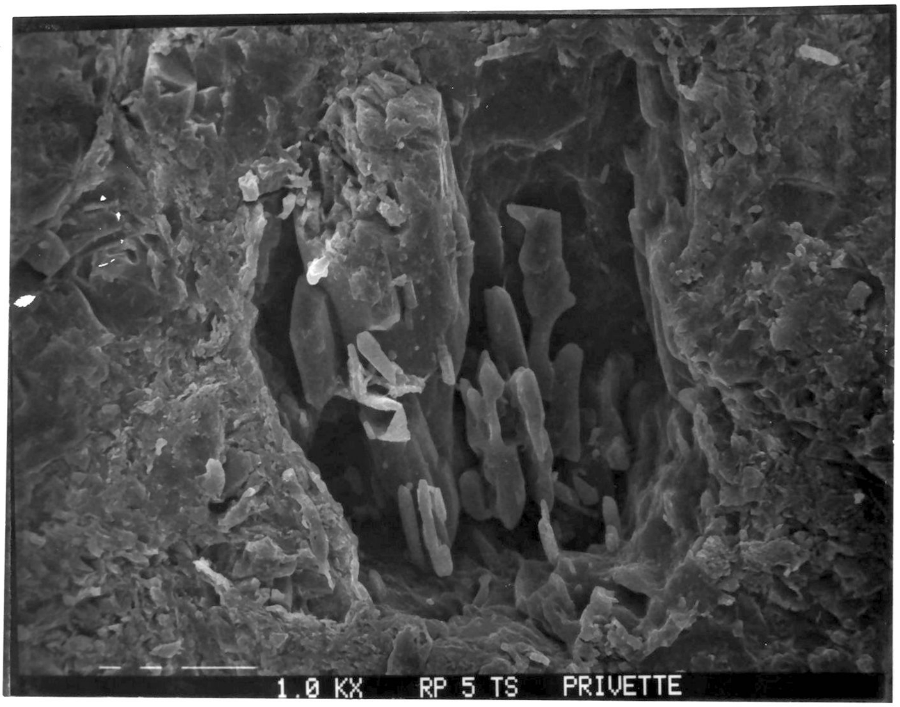

Figure 18. SEM photo of altered feldspar showing inplace dissolution of the grain and the formation of intraparticle secondary porosity. (1000x)

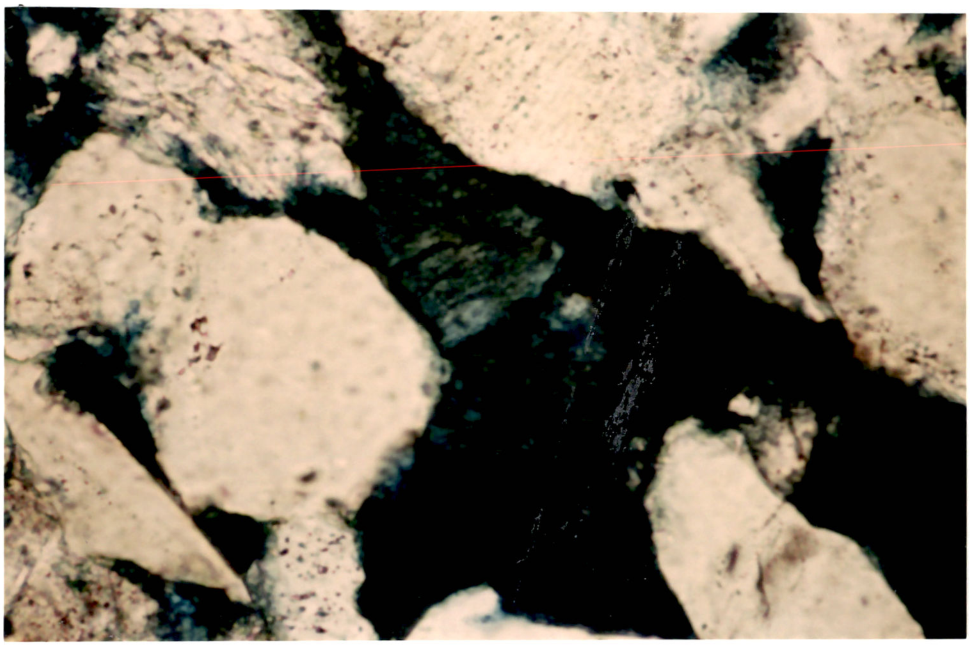

Figure 19. Intraparticle secondary microporosity in a shale clast. Also minor fracture porosity. Blue is colored epoxy. Plane light. (630x)

clasts. Although these clasts are common, the amount of total or effective porosity created is insignificant.

Pore Casts

The study of pore casts provides information on the distribution and shape of pores and pore throats. Figure 20 shows the continuous pore network of lamellar porosity (Schmidt and McDonald, 1979) that surrounds the grains. This irreducible, fluid filled porosity is necessary for diagenesis and is found in all samples regardless of the porosity. An example of this porosity can be seen as the space between the fibrous illite and the quartz in Figure 24. The small size of the pore throats shows why the permeability is very low throughout the Weir even in samples with relatively high porosity.

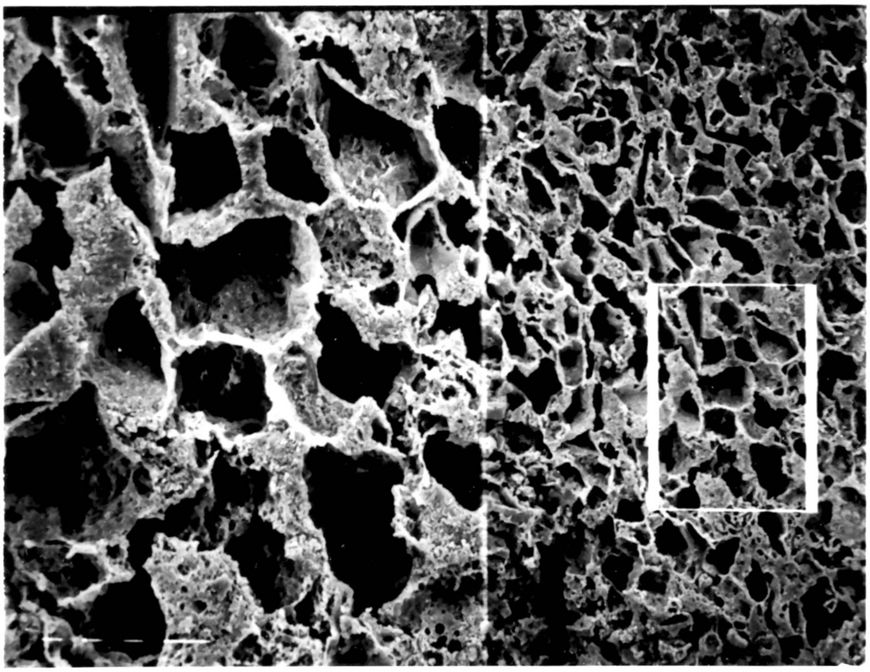

Figure 20. SEM photo of pore casts. Voids show area occupied by grains and epoxy shows pore space. The right side of the photo is shown at 60x and the portion within the square is shown on the left at 180x. The longest bar in the bar scale represents 100 microns.

Factors Affecting Porosity

Variations in the porosity and permeability of the Weir are due to the alteration of original porosity by diagenetic processes. These processes may be separated into three groups: (1) factors which tend to reduce porosity; (2) factors which tend to preserve porosity; and (3) factors which tend to increase porosity.

Factors Reducing Porosity

The two most important factors in reducing porosity are compaction and the formation of authigenic minerals. Compaction by overburden pressure results in a significant reduction of the initial porosity by causing closer grain packing and by deforming ductile grains.

An estimate of porosity lost due to compaction can be computed using an estimated percentage of original porosity, the percentage of detrital grains, and the percent porosity now present. Prior to compaction, the initial porosity of a fine-grain sand is 35 to 40% (Hayes, 1979). In the Weir the mean percentage of detrital grains (72%) gives a value of approximately 28% for post-compaction porosity, which equates to approximately 75% of the total initial porosity. Hence, 25% of the initial porosity was lost due to compaction. As compaction continues, ductile grains are deformed by rigid grains as they become closely packed and can no longer shift positions to accommodate stress. Figure 21 is taken from a study by Rittenhouse (1971) in which he attempted to compute the reduction in porosity due to the deformation of ductile

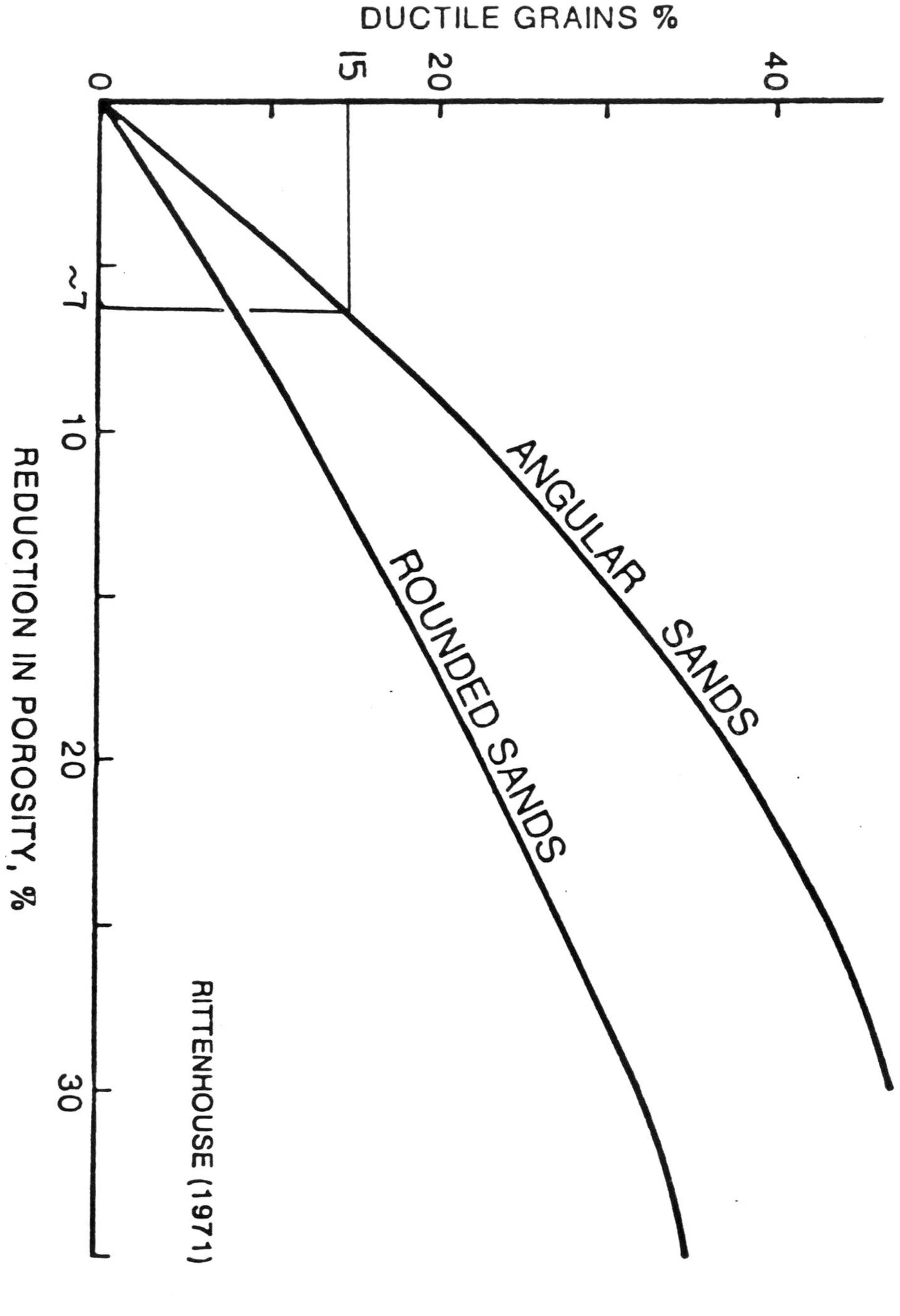

Figure 21. Curves showing loss of porosity due to various percentages of ductile grains present in rounded and angular sand. Modified after Rittenhouse (1971).

grains. The percentage of ductile grains in the Weir is approximately 15%. The ductile grains are primarily rock fragments, minus the chert and quartzite fragments. This percentage of ductile grains, when plotted on the curve, corresponds to a 7% loss in total porosity due to ductile grain deformation. With continuing compaction after ductile grain deformation, the quartz grains undergo pressure solution at grain contacts. Although evidence for pressure solution is common, it has only a minor effect on porosity reduction.

The formation of authigenic minerals is the second major cause of porosity reduction. Authigenic quartz, clays, carbonates, and sulfates, which comprise approximately 12% of the samples, reduce porosity because they form primarily in pores, either as pore fillings or as pore linings. Carbonate pore fillings are found throughout the Weir and significantly reduce porosity in its lower portion. Sulfates are found primarily in the lower portion and quartz overgrowths are found throughout the Weir, but neither significantly reduces porosity. Authigenic clays reduce both porosity and permeability, and each of the clays affects the porosity in a different way.

Chlorite is the most important authigenic clay. It forms pore linings which not only reduce porosity but also severely reduce permeability. These pore linings are found primarily in the upper portion of the Weir where they impede the flow of fluids through pore throats. The chlorite forms radially oriented crystals projecting into pore spaces from grain surfaces, slightly reducing intergranular porosity but greatly reducing permeability by decreasing the cross-sectional area of the pore throats (Fig. 22). Calculations by Galloway (1979) shows that a 4% increase in grain diameter by clay coatings on close packed spheres causes a 26% reduction in pore throat diameter. Since the Weir has a mean grain size of 0.116 mm and the mean thickness of the chlorite coatings is approximately 0.007 mm, the resulting increase in grain diameter would be roughly 6%. Because the permeability is proportional to the square of the pore throat diameter, the permeability would be significantly reduced by the 6% increase in grain diameter. The decrease in pore throat diameter reduces permeability by increasing the surface area within the pore throat. The increase in surface area is due to the large surface-to-volume ratio of the platy clay crystals (Blatt, 1982). These clay crystals increase the amount of viscous drag on the fluid as it passes through the pore throat.

Kaolinite accounts for a very small reduction in porosity since it occurs primarily as an in situ replacement of K-feldspar. Kaolinite also occurs as rare clusters of euhedral crystals filling pore space in the upper portion of the unit. The crystals are uncommon, and their effect on porosity is negligible.

Authigenic illite comprises less than 1% of the bulk rock and occurs as thin coatings on quartz grains. The small quantities and tangential orientation of the illite would not significantly reduce porosity or permeability.

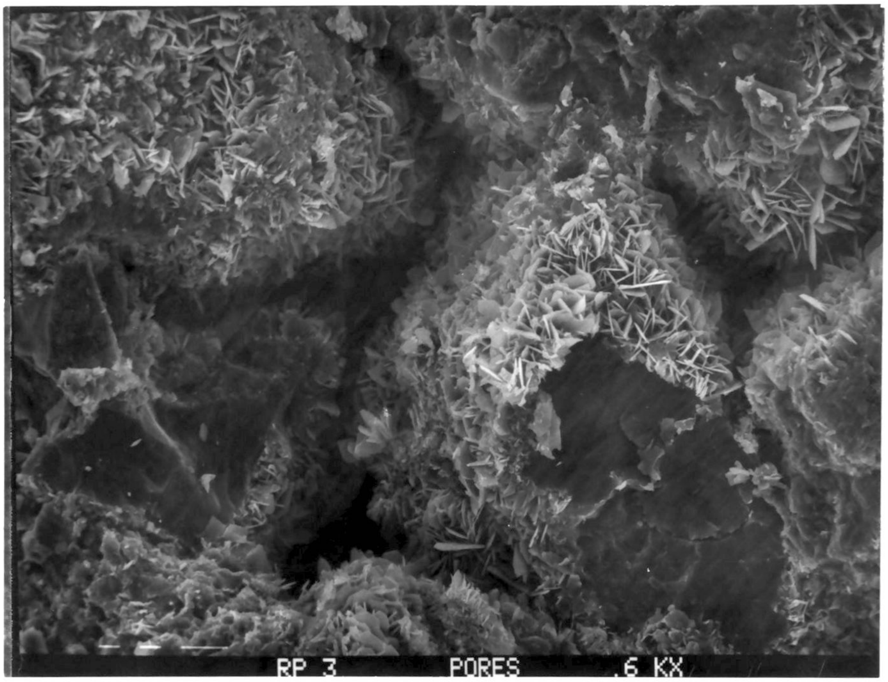

Figure 22. SEM photo of chlorite grain coating. Note the thick, well crystallized chlorite grain coating and narrow pore throats. (600x) Longest bar on bar scale represents 100 microns.

Factors That Preserve Porosity

Previous investigations by Heald (1965), Cecil (1966), and Pittman and Lumsden (1968) have shown the effectiveness of authigenic clay coatings in preventing the formation of secondary quartz. The chlorite grain coatings present in the Weir have preserved porosity by preventing the precipitation of authigenic quartz that would have significantly reduced porosity during the late stage of diagenesis. The silica is prevented from forming overgrowths because of a lack of nucleation sites on the quartz grains.

Factors That Increase Porosity

Porosity has been increased by the formation of secondary porosity. The secondary porosity was created by the dissolution of detrital grains, primarily feldspar and calcite. Only a small percentage of the feldspar has undergone sufficient dissolution to produce porosity and it is doubtful that it could contribute significantly to the effective porosity. The dissolution of first generation (early diagenetic) calcite may have significantly increased porosity. Since there is no way to estimate the abundance of early calcite, it is impossible to determine the amount of porosity created by its dissolution.

DIAGENETIC SEQUENCE

The diagenetic sequence proposed for the Weir (Figure 23) can be separated into three stages: early, middle, and late diagenesis. Early diagenesis is characterized by compaction of the sediment and the formation of authigenic minerals. The first authigenic mineral to form was pyrite, which forms in a reducing environment from ferrous iron and sulfur derived from organic materials (Love, 1971). Concurrently with or shortly after the pyrite formation, the first generation of calcite formed from carbonate material available near the sediment-water interface. The calcite formation was followed by the formation of siderite and illite. The siderite formed in an environment similar to the calcite but with more abundant ferrous iron available (Dapples, 1975). Since siderite is common only to samples in proximity to interbedded shales, the shales probably were the source of the iron. Examples of siderite replacing calcite show that siderite formed after the calcite. Illite formed as an irregular coating on quartz grains and the delicate, fibrous coatings indicate an authigenic origin (Fig.24). The conditions that formed the illite would also begin to alter the smectite and mixed-layer (illite-smectite) clays in rock fragments and matrix material. This alteration process would be continuous through the late stage of diagenesis when temperatures would become high enough to transform the mixed-layer clays to illite.

The middle stage of diagenesis is characterized by the formation of quartz overgrowths, the dissolution of authigenic minerals and detrital

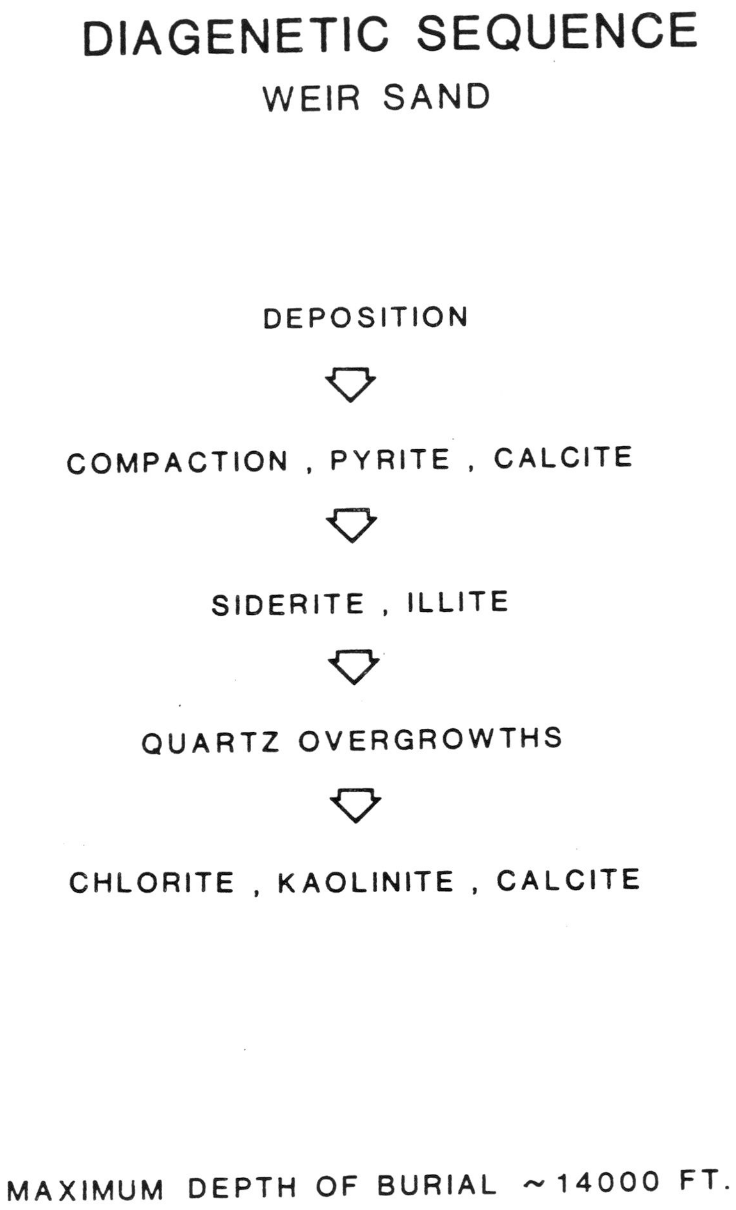

Figure 23. Proposed diagenetic sequence.

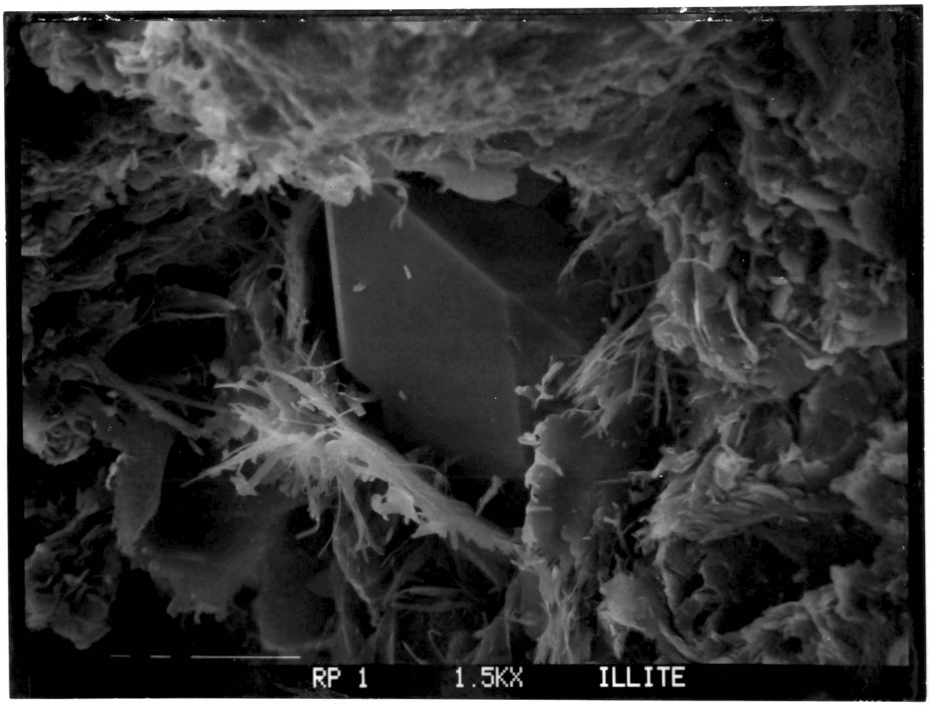

Figure 24. Authigenic illite surrounding quartz(?) overgrowth. SEM photo. (1500x) The longest bar in the bar scale represents 10 microns.

grains, and the formation of secondary porosity. This shift from precipitation to dissolution is due to a change from reducing to oxidizing conditions within the Weir. With increasing pressure and temperature, and the presence of authigenic illite, pressure solution of quartz would put free silica into the system. Free silica would also be derived from other sources such as carbonate-quartz contacts, alteration of feldspars, and the transformation of smectites to illite (Foscolos and Powell, 1979). Free silica would form secondary quartz overgrowths which occur as optically continuous syntaxial overgrowths and as overgrowths with a polygonal grid texture. The inclusion of illite in the polygonal overgrowths shows that illite formation preceded and/or was synchronous with the overgrowth (Fig.25).

Secondary porosity formed during the middle stage by dissolution of calcite, feldspar, and rock fragments. The dissolution of calcite created an indeterminable amount of intergranular porosity and the dissolution of detrital grains created minor amounts of such porosity. The alteration of feldspar also released silica and cations. The release of potassium ions (K^+) during kaolinization of potassium feldspar was important in the transition of smectite to illite. This transition affected the porosity by releasing interlayered water from the smectite. The water released would be acidic (Johns and Shimoyama, 1972) and would decrease the pH and cause a shift from reducing to oxidizing conditions in the pore fluids. The change in pore fluid chemistry would lead to the formation of secondary porosity due to the dissolution of calcite and detrital grains. Acidic waters may also have been derived from the

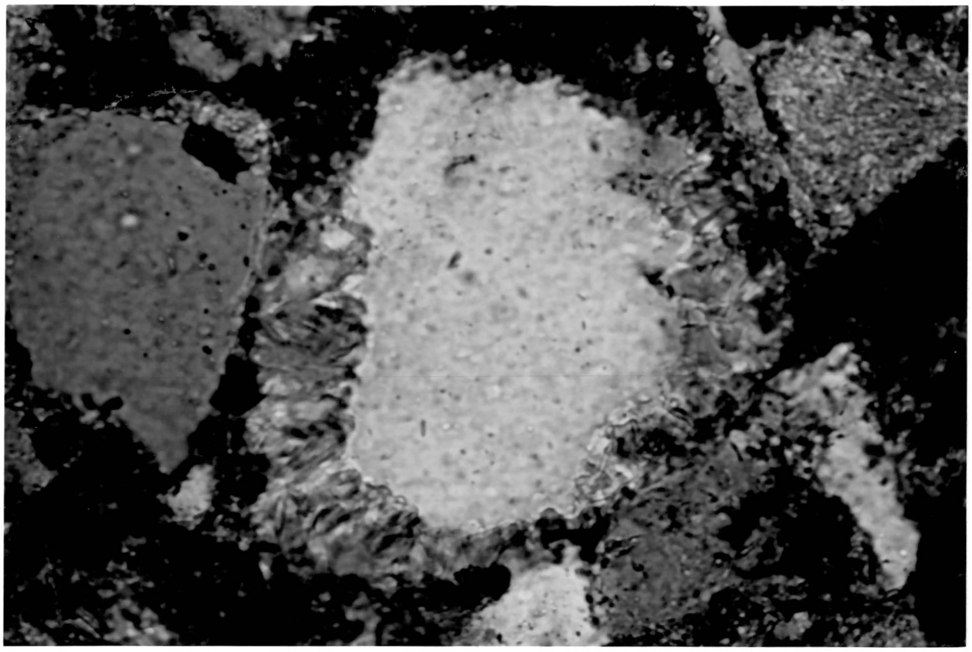

Figure 25. Polygonal overgrowth on quartz. Authigenic illite is shown by the high birefringent grains incorporated in the authigenic quartz. Partially crossed nicols. (630x)

transition of smectite in adjacent shale strata. The acidity would have been increased not only by the ions in the clay water but also by the addition of carbon dioxide from the decarboxylation of organic material in the shales. The association of hydocarbon formation with the smectite to illite transformation has beem demonstrated by Johns and Shimoyama (1972) and Foscolos and Powell (1979). Hydocarbon migration into the Weir probably occurred concurrently with the clay transformation and was prompted by the increase in pore fluid pressure accompanying the release of interlayered water in the smectite. The alteration of smectites and mixed-layer clays would explain why large amounts of well crystallized illite are found in the Weir, but only traces of mixed-layer clay are present. The smectites would be transformed to illite at a temperature of 65° to 75°C and this temperature was probably reached during the middle stage (Dypvik, 1983). The mixed-layer clays require higher temperatures (80° to 100°C) for complete transformation to illite and would be altered during the late stage of diagenesis. Evidence for the middle stage migration of hydrocarbons into the Weir is also shown by the very low permeability of the sand. The migration occurred prior to the formation of late stage chlorite grain coatings, which restricted pore throats by reducing permeability and sealed the hydrocarbons in the pores. The fact that gas is sealed in the pores is shown by the low initial flow of producting wells. The initial production from gas wells produces only traces of hydrocarbons, but after fracturing to increase the permeability, large volumes of gas are produced.

The late stage of diagenesis is recognized by the formation of chlorite, calcite, sulfates, and kaolinite. The chlorite forms thick grain coatings which act as cement and slightly reduce porosity but greatly reduce permeability. The origin of authigenic chlorite is not well understood and several theories have been offered. Thompson (1970) stated that chlorite is formed when ferrous iron is absorbed by degraded phyllosilicates under reducing conditions. He also stated that iron-rich chlorite and 1M illites are indicative of this process. Conditions in the Weir are compatible with this sequence because iron-rich chlorite and 1M illite are the most common types of these minerals. Larese (1974) postulated that chloritic material was scoured from channels and put into colloidal suspension. This material was then trapped in the sediments and precipitated as chlorite under reducing conditions. Powers (1957) stated that chlorite could form from the alteration of illite under marine conditions. The mechanism for chlorite formation in the Weir is not known, but any one or a combination of these sources may be responsible for the origin of the chlorite. The only common denominator in these theories is that chlorite formation requires a reducing environment. The shift from an oxidizing environment in the middle stage to a reducing condition caused the formation of a second generation of calcite. The calcite formed pore fillings and commonly had a poikilotopic texture (Fig.26). By the late stage of diagenesis, K-feldspar would have been leached of its K^+ and its silica and the remaining material would be predominantly kaolinite. Evidence for the feldspar retaining its original form through the early and middle stages

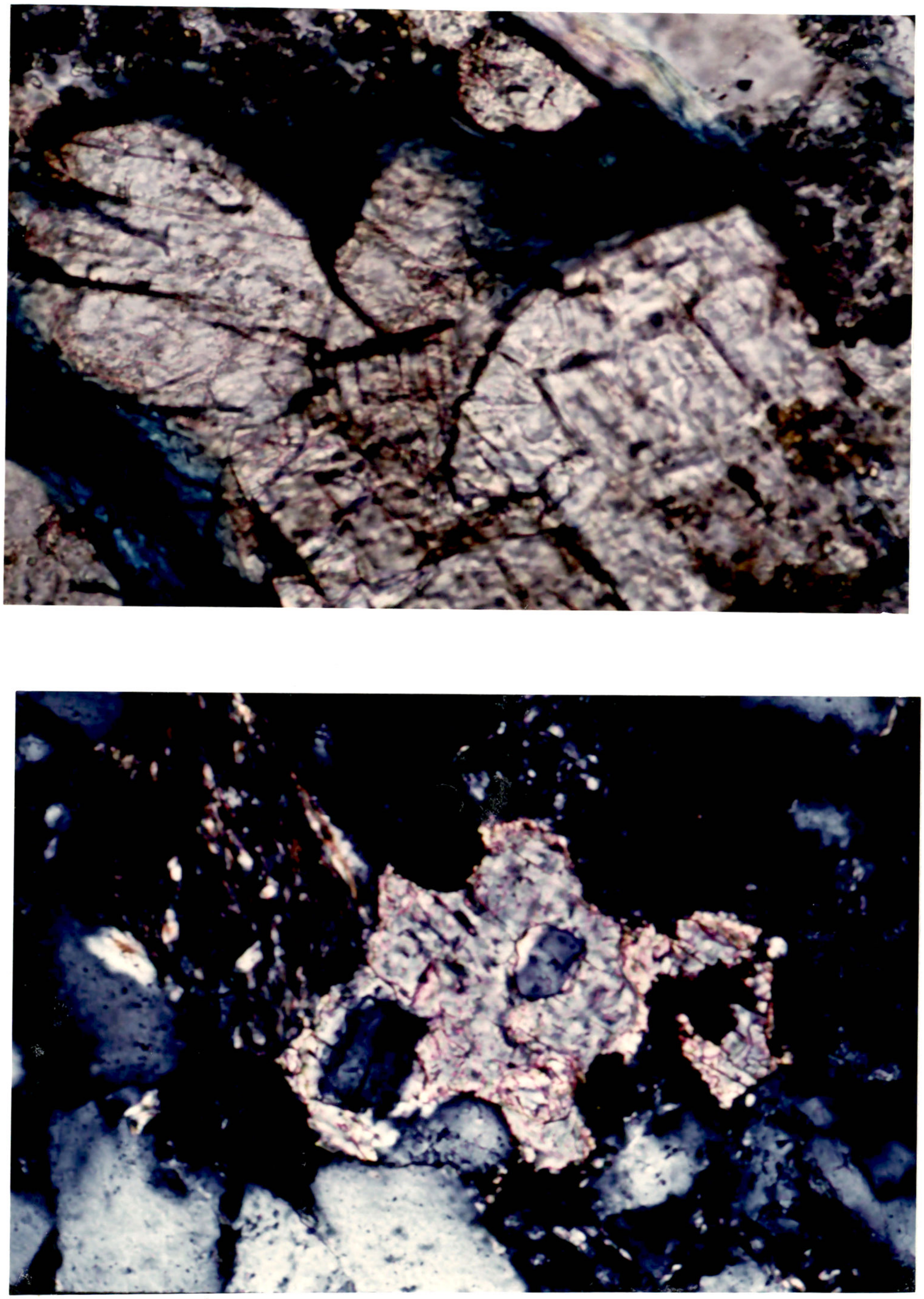

(A)
(630x)

(B)
(250x)

Figure 26. (A) First generation of authigenic calcite. (B) Second generation of authigenic calcite. In photo (A) note the rounded edges, broken grain, and pore space around the calcite. In photo (B), note the irregular angular shape.

can be seen in Figure 27. The figure shows the feldspar completely replaced by kaolinite. However, the original feldspar shape has not been deformed by compaction during the earlier diagenetic stages.

Minor amounts of anhydrite and barite also formed during the late stage, apparently as a replacement of calcite. Blount and Dickson (1969) found that anhydrite precipitation occurred when ion-saturated solutions migrated from areas of high pressure to areas of lower pressure and the high-ionic strength solution contacted fresher waters. The solutions probably migrated from underlying shales since the sulfates are found predominantly in the lower portion. The rare dolomite rhombs found in the Weir probably formed during late diagenesis from Mg^{++} released by the transformation of mixed-layer clay to illite.

The mixed-layer clays were not transformed to illite until the late stage of diagenesis when the depth of burial was sufficient to produce temperatures of at least 80° to 100°C and the geochemical conditions were present that are necessary for the transformation (Dypvik, 1983). This temperature can be derived using the maximum depth of burial postulated for the Weir (12,000-14,000 ft; 3,650-4270 m) and the standard estimate of the geothermal gradient (25° per kilometer). The minimum estimated temperature for transformation is approximately 106°C. This temperature would be sufficient to transform the mixed-layer clays to illite, but the maximum temperature could have been greater due to a higher geothermal gradient in the study area.

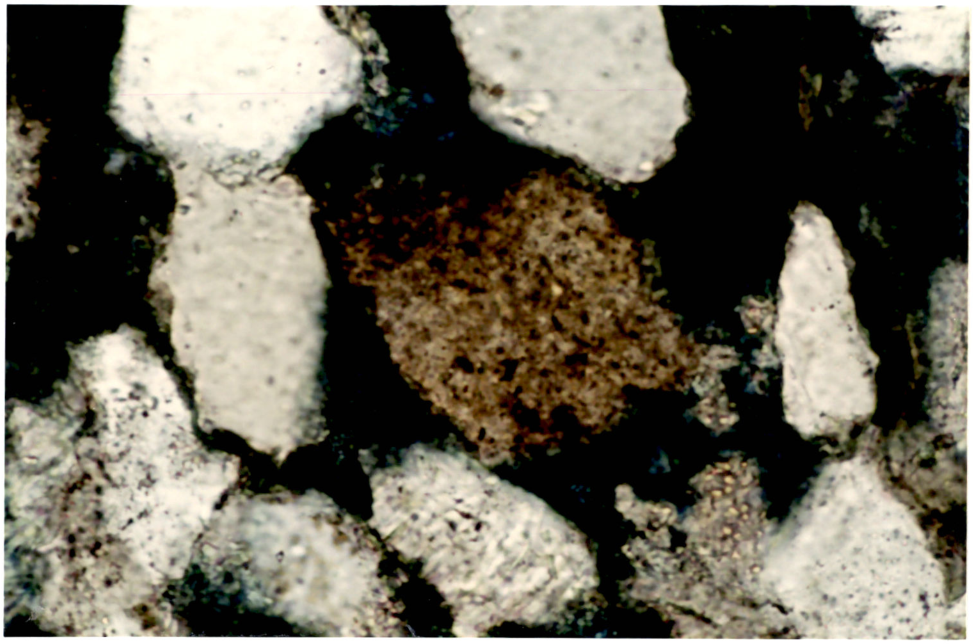

Figure 27. Brown grain is altered K-feldspar. Note the lack of deformation of the grain even at contacts with quartz grains. Plane light. (250x)

SUMMARY AND CONCLUSIONS

In the Ashland-Clark Gap gas field, the Weir sand is a fine to very fine-grained lithic arenite. The lithic fragments, which are predominantly SRFs with minor MRFs, suggest a combined metamorphic (greenschist facies) and sedimentary source area. XRD studies of the clay sized fraction indicate a clay mineral suite of illite, kaolinite, chlorite, and mixed-layer clays. Kaolinite and illite are the dominant clay minerals. Kaolinite formed from the alteration of detrital K-feldspars and the illite represents both detrital illite and authigenic illite formed by the transformation of smectite and mixed-layer clays in shale clasts and matrix material. Chlorite formed from solution as a grain coating and is far less abundant by volume than illite or kaolinite.

Porosity in the Weir is predominantly intergranular primary porosity that has been reduced in volume by authigenic chlorite grain coatings. Approximately 10% of the total porosity is intergranular and intragranular secondary porosity. This porosity was created by the dissolution of detrital grains, primarily feldspar and lithic fragments, and calcite. The porosity in the Weir has been affected by several processes which include, in decreasing order of importance: (1) processes that reduce porosity; (2) processes that preserve porosity; and (3) processes that increase porosity. The greatest effect on porosity has been its overall reduction by compaction, ductile grain deformation, and the formation of authigenic minerals. Compaction had the greatest effect in reducing the initial porosity. The formation of authigenic minerals, primarily calcite, siderite, and chlorite, also had a major effect on reducing porosity. Ductile grain deformation significantly reduced porosity due to the large percentage of easily deformed lithic fragments in the Weir. Porosity was preserved in the Weir by chlorite grain coatings which obscured nucleation sites on the quartz grains and prevented the formation of secondary quartz overgrowths during the late stage of diagenesis. Porosity was only slightly increased by the formation of secondary porosity. This porosity was created by the dissolution of calcite, feldspars, and lithic fragments.

The diagenetic sequence in the Weir can be divided into early, middle, and late stages. The early stage began with the initial compaction of the sediments and the formation of pyrite and calcite. This was followed by the formation of grain coating illite and pore filling siderite. The middle stage of diagenesis was characterized by the formation of quartz overgrowths and the creation of secondary porosity due to changes in the geochemical conditions. The late stage of diagenesis was characterized by the formation of chlorite grain coatings, the alteration of K-feldspar to kaolinite, and the formation of a second generation of calcite pore filling. The chlorite and calcite formations indicate a change in geochemical conditions from oxidizing conditions in the middle stage to reducing conditions in the late stage.

Statistical analysis of the constituents show several significant trends. The most significant trend, shown by correlation coefficients, is the reduction in porosity due to increasing percentages of calcite and siderite. R-mode factor analysis suggests this trend also. The factor analysis suggests that 2 factors account for the majority of the variance found in the samples. The first factor accounts for 63% of the variance and consists of the variables calcite and siderite. The second factor accounts for 24% of the variance and consists of the variables matrix and porosity. The remaining 13% is divided among three factors and does not account for a significant amount of variance in any one factor.

REFERENCES CITED

Ashburner, C. A., 1876, Report of the Aughwick Valley and East Broad Top district: Pennsylvania Second Geological Survey, Report F, p. 141-288.

Bartlett, C. S., Jr., 1974, Anatomy of the Lower Mississippian Delta in Southwest Virginia: unpublished PhD dissertation, University of Tennessee, 452p.

Biscaye, P. E., 1964, Distinction between kaolinite and chlorite in recent sediments by X-ray diffraction: American Mineralogist, v. 49, p. 1281-1289.

Blatt, Harvey, 1979, Sedimentary Petrology, San Francisco, W. H. Freeman and Co., 564p.

Blount, C. W. and Dickson, F. W., 1969, The solubility of anhydrite in NaCl from 100° to 450°C and 1 to 1,000 bars: Geochimica et Cosmoschimica Acta, v. 33, p.

Boggs, Sam, Jr., 1968, Experimental study of rock fragments: Journal of Sedimentary Petrology, v. 38, p. 1326-1339.

Boone, G. M., and Wheeler, E. P., 1968, Staining for cordierite and feldspar in thin-section: American Mineralogist, v. 53, p. 327-331.

Branson, E. B., 1912, A Mississippian delta: Geologic Society of America Bulletin, v. 23, p. 447-456.

Briggs, Garrett, 1974, Carboniferous of the Southeastern United States: Geologic Society of America, Special Paper 148, 361p.

Butts, Charles, 1940, Geology of the Appalachian Valley in Virginia, Part I: Virginia Geological Survey Bulletin, No. 52, 568p.

Campbell, M. R., 1894, Paleozoic overlaps in Montgomery and Pulaski Counties, Virginia: Geological Society of America Bulletin, v. 5, p. 171-190.

Carrigy, M. A., and Mellon, G. B., 1964, Authigenic clay mineral cement in Cretaceous and Tertiary sandstones of Alberta: Journal of Sedimentary Petrology, v. 34, p. 461-472.

Carrol, Dorothy, 1970, Clay minerals: A Guide to their X-ray identification: Geological Society of America, Special Paper No. 126, 80p.

Cecil, C. B., 1966, The effects of coatings on quartz growth: Unpublished M.S. thesis, Morgantown, West Virginia University, 38p.

Chadwick, G. H., 1935, What is "Pocono?": American Journal of Science, v. 29, p. 133-143.

Chayes, Felix., 1956, Petrographic modal analysis: New York, John Wiley and Sons, Inc., 133p.

Choquette, P. W., and Pray, L. C., 1970, Geological nomenclature and classification of porosity in sedimentary carbonates: Bulletin of the American Association of Petroleum Geologist, v. 54, p. 207-250.

Cooper, B. N., 1948, Status of Mississippian stratigraphy in the central and northern Appalachian region: Journal of Geology, v. 56, p. 255-263.

Dally, J. L., 1956, Stratigraphy and paleontology of the Pocono Formation in West Virginia: Unpublished PhD dissertation, New York, Columbia University, 241p.

Davis, M. W., and Ehrlich, Robert, 1974, Late Paleozoic crustal composition and dynamics in the southeastern United States: Geologic Society of America, Special Paper No. 148, p. 171-186.

Dypvik, Henning, 1983, Clay mineral transformations in Tertiary and Mesozoic sediments from the North Sea: American Association of Petroleum Geologist, v. 67, p. 160-165.

Folk, R. L., 1974, Petrology of Sedimentary Rocks: Austin, Hemphill Publishing Co., 185p.

Fontaine, W. M., 1877, Notes on the Vespertine strata of Virginia and West Virginia: American Journal of Science, 3rd. Series, v. 13, p. 37-48.

Foscolos, A. E., and Powell, T. G., 1979, Mineralogical and geochemical transformations of clays duting burial diagenesis (catagenesis); relation to oil generation: Developments in Sedimentology, v. 27, p. 261-270.

Furbish, W. J., 1974, Polished thin sections for cathode-luminescent study: Nuclide Corp. Publication No. 1488.

Galloway, W. E., 1979, Diagenesis control of reservoir quality in arc-derived sandstones: implications for petroleum exploration, In, P. A. Scholle and P. E. Schluger, eds., Aspects of diagenesis: Society of Economic Paleontologists and Mineralogists, Special Publication No. 26, p. 251-262.

Gardner, K. L., 1980, Pressure impregnation of thin section: Canadian Journal Earth Science, v. 17, p. 907-910.

Glover, Lynn, 1953, The stratigraphy of the Devonian-Mississippian boundary in southwestern Virginia: M.S. thesis, Blacksburg, Virginia Polytechnic Institute and State University v. 2, p. 71-78.

Grayson, J. F., 1956, The conversion of calcite to fluorite: Micropaleontology, v. 2, p. 71-78.

Grim, R. E., Bradley, W. F., and Brown, G., 1951, The mica clay minerals, In Brindly, G. W., ed., X-ray identification and crystal structure of the clay minerals: Mineralogical Society of London, p. 138-172.

Hayes, J. B., 1979, Sandstone diagenesis - the hole truth, In Scholle, P. A., and Schinger, P. R., eds., Aspects of diagenesis: Society of Economic Paleontologists and Mineralogists Special Publication No. 26, p. 127-139.

Heald, M. T., 1972, Lithification of sandstones in West Virginia: West Virginia Geologic and Economic Survey Bulletin No. 30, 28p.

Kerisa, R. D., 1972, The origin of the Price Formation in the type area, Montgomery and Pulaski Counties, Virginia: Unpublished M.S. Thesis, Blacksburg, Virginia Polytechnic Institute and State University, 65p.

Larese, R. E., 1974, Petrology and stratigraphy of the Berea Sandstone in the Cabin Creek and Gay-Fink Trends: Unpublished PhD dissertation, Morgantown, West Virginia University, 246p.

Love, L. G., 1971, Early diagenetic polyframboidal pyrite, primary and redeposited, from the Wenlockian Denhigh Grit Group, Conway, North Wales, U.K.: Journal of Sedimentary Petrology, v. 41, p. 1038-1044.

Miyashairo, Akiho, 1973, Metamorphism and Metamorphic Belts; New York, John Wiley & Sons, 492p.

Pelletier, B. R., 1958, Pocono paleocurrents in Pennsylvania and Maryland: Geological Society of America Bulletin, v. 59, p. 1033-1064.

Pepper, J. F., de Witt, Wallace, Jr., and Demarest, D. F., 1954, Geology of the Bedford Shale and Berea Sandstone in the Appalachian Basin: United States Geological Survey Professional Paper No. 259, 109p.

Perry, E. A., and Hower, John, 1970, Burial and diagenesis in Gulf Coast pelitic sediments: Clay and Clay Minerals, v. 18, p. 165-177.

_______ and Dushatko, R. W., 1970, Use of pore casts and the scanning electron microscope to study pore geometry: Journal of Sedimentary Petrology, v. 4, p. 1153-1157.

_______ and Lumsden, D. N., 1968, Relationships between chlorite coatings on quartz grains and porosity, Spiro Sand, Oklahoma: Journal of Sedimentary Petrology, v. 38, p. 668-670.

Powers, M. C., 1957, Adjustment of land derived clays to the marine environment: Journal of Sedimentary Petrology, v. 27, p. 353-372.

Reger, D. B., 1926, County Reports for Mercer, Monroe, and Summers Counties: West Virginia Geological Survey County Reports, 963p.

Rittenhouse, Gordon, 1971, Mechanical compaction of sands containing different percentages of ductile grains: a theoretical approach: Bulletin of the American Association of Petroleum Geologist, v. 55, p. 92-96.

Rogers, W. B., 1838, Report on the progress of the Geological Survey of the state of Virginia for the year of 1837: Richmond, Virginia, 24p.

Schmidt, Volkmar and McDonald, D. A., 1979, The role of secondary porosity in the course of sandstone diagenesis: In Scholle, P. A. and Schluger, P. R., eds., Aspects of diagenesis: Society of Economic Paleontologists and Mineralogists Special Publication No. 26, p. 175-207.

Scholle, P. A., 1979, A color illustrated guide to consituents, textures, cements, and porosities of sandstones and associated rocks: American Association of Petroleum Geologist Memoir 28.

Stevenson, J. L., 1903, Lower Carboniferous of the Appalachian basin: Geological Society of America Bulletin, v. 14, p. 16-45.

Thompson, A. M., 1970, Geochemistry of color genesis in red bed sequence, Juanita and Bald Eagle Formations, Pennsylvania: Journal of Sedimentary Petrology, v. 40, p. 599-615.

Thorez, Jacques, 1976, Practical identification of clay minerals: G. Lelotte, Belgium, 89p.

Ulman, N. P., 1978, Elementary statistics: New York, John Wiley & Sons, 372p.

Van der Plas, L., 1975, Identification of detrital feldspar: Developments in sedimentology, v. 6, New York, Elsvier, 305p.

_______ and Tobi, A. C., 1965, A chart for judging the reliability of point counting results: American Journal of Science, v. 263, p. 87-90.

Walker, K. R., 1964, Price-Pocono stratigraphy of southwest Virginia: Masters Thesis, Chapel Hill, University of North Carolina, 74p.

Weyl, P. K., 1959, Pressure solution and the force of crystallization - A phenomenological theory: Journal of Geophysical research, v. 64, p. 2001-2025.

Williamson, N. L., 1974, Depositional environment of the Pocono Formation in southwest West Virginia: Unpublished PhD dissertation, Morgantown, West Virginia University, 171p.

Woodward, H. P., 1932, Geology and mineral resources of the Roanoke area, Virginia: Virginia Geological Survey Bulletin, v. 34, 172p.

APPENDIX A

Statistical Analysis

Statistical analysis was performed using SPSS-9 (Statistical Package for Social Science, version 9). The analysis included descriptive statistics, correlation coefficients, and R-mode factor analysis for the upper, lower, and combined Weir samples. The primary function of the analysis was to determine which constituents (variables) influenced changes in the petrology and porosity. A separate analysis was performed on the clay fraction to determine the effects of clay abundance on the porosity.

The Pearson product moment correlation coefficient (r) was used to determine if a significant relationship existed between the percentage of both quartz and porosity and the percentages of feldspar, calcite, siderite, rock fragments, and matrix for 33 Weir samples. The correlation coefficient has a minimum and maximum value of -1.0 and 1.0, respectively, and indicated the degree of correlation for values of two variables when plotted on the X and Y axes of a scatter diagram. A value of 1 would be a perfect correlation with all points plotted on a straight line and the sign of the value would indicate the slope of the line. A value of 0 would indicate there is no correlation between the variables. The minimum value of r for it to be considered significant, the critical value, is based on the number of samples and the level of confidence desired. For this study, 33 samples were used and a confidence level of

0.01 was chosen. Using a table of critical values for correlation coefficients by Ulman (1978), the critical value for this study would be r = 0.488. This value indicates that any value of r greater than 0.488 has a greater than 99% probability of showing a significant relationship between two variables. For the study of the clay fraction, a separate critical value was used due to a change in sample size. For 21 samples at a 0.01 confidence level, the critical value would be r = 0.537.

Correlation coefficients show that the only variable in the combined samples with a significant effect on porosity is calcite (Table 1). The negative r value suggests a significant reduction in porosity as the percentage of calcite increases. The negative r value for siderite suggests a significant reduction in quartz as the percentage of siderite increases. Correlation coefficients were also computed for the clay fraction and compared to porosity. The values for the clays were derived from estimates of clay abundance using XRD patterns.

The r values for chlorite and kaolinite show a significant relationship between the clays and porosity. Values of r = 0.688 for chlorite and r = 0.746 for kaolinite indicate an increase in chlorite and kaolinite abundance with increasing porosity. This relationship is due to the increased availability of pore fluids as porosity increases. These fluids are primarily responsible for the alteration of K-feldspar to kaolinite and for the formation of chlorite from solution. The low, negative value of illite (r = -0.002) is significant and is probably due to illite being found in abundance throughout the Weir in shale clasts and matrix.

Factor analysis is a method of data reduction used to analyze interrelationships within a set of variables. Factors are established that contain the essential information of the larger set of observed variables. The factors are constructed in a way that reduces the overall complexity of the data by taking advantage of the inherent interdependencies within the data. As a result, a few factors will usually account for approximately the same information as does the much larger set of original data. The study used R-mode factor analysis, which analyzes the relationships among constituents (variables) and not between samples.

Table A3 lists the factors selected by the analysis. The primary factor, Factor #1, for the combined samples shows that calcite and siderite account for 63.6% of the variation in the samples. In the upper portion quartz is a significant variable, while in the lower portion rock fragments are significant. This large amount of variation attributed to the carbonates is probably due to their local abundance in the lower portion. Factor #2 consists of porosity and matrix and a accounts for 23.7% of the variation. The variation can be attributed to major differences in porosity of the upper and lower portion and an interface in matrix material in the lower portion. Factor #3 for the combined samples accounts for 8.2% and shows the variation is distributed among several variables with none of them contributing significantly to the variation. The remaining 4.5% of variation is accounted for by Factors #4 and #5, Table A4, and no variables appear to be significant.

Overall, the statistical analysis indicates that calcite and siderite are the most important variables. They account for most of the variation in the samples and are inversely related to both quartz and porosity abundance.

TABLE A1
CORRELATION COEFFICIENTS

	Quartz	Porosity
Feldspar	0.082	0.451
Rock Fragments	0.423	0.217
Calcite	-0.453	-0.554
Siderite	-0.515	-0.460
Porosity	-0.003	1.000
Matrix	-0.325	-0.482
Quartz	1.000	-0.003

Combined Weir samples. Only coefficients greater than 0.488 are considered significant.

TABLE A2
CORRELATION COEFFICIENTS

	Quartz	Porosity
Feldspar	0.260	0.159
Rock Fragments	0.493	0.281
Calcite	-0.570	-0.317
Siderite	-0.604	-0.237
Porosity	0.080	1.000
Matrix	0.302	-0.384
Quartz	1.000	0.080

Lower Weir Samples. Only coefficients greater than 0.557 are considered signinicant.

	Quartz	Porosity
Feldspar	-0.125	0.616
Rock Fragments	0.387	-0.302
Calcite	-0.491	-0.401
Siderite	-0.557	-0.366
Porosity	0.271	1.000
Matrix	0.354	0.209
Quartz	1.000	0.659

Upper Weir Samples. Only coefficients greater than 0.574 are considered significant.

TABLE A3
Factor Analysis

Combined Weir Samples	% Variation
Factor #1 - Siderite, Calcite	(63.6%)
Factor #2 - Porosity, Matrix	(23.7%)
Factor #3 - (none significant)	(8.2%)
Upper Weir Samples	
Factor #1 - Quartz, Calcite, Siderite	(44.0%)
Factor #2 - Feldspar, Porosity, Rock Fragments	(32.0%)
Factor #3 - Quartz, Matrix	(14.0%)
Lower Weir Samples	
Factor #1 - Calcite, Siderite, Rock Fragments	(64.4%)
Factor #2 - Matrix, Porosity	(20.9%)
Factor #3 - Quartz	(8.2%)

Significant variables from factor analysis matrix. Percent variation shows the percentage of variation that can be attributed to each factor. Variables are listed in order of decreasing value.

TABLE A4

R-Mode Factor Analysis
Combined Weir Samples

Factor Matrix using Principal Factor With Iterations

	Factor 1	Factor 2	Factor 3	Factor 4	Factor 5
Quartz	0.481	0.378	-0.300	-0.237	0.015
Feldspar	0.505	-0.275	-0.309	-0.192	0.007
Porosity	0.609	-0.629	0.009	0.128	0.023
Rock Fragments	0.646	0.314	-0.183	0.228	0.030
Calcite	-0.909	-0.016	-0.007	0.002	0.179
Siderite	-0.941	-0.226	-0.161	0.000	-0.126
Matrix	-0.153	0.596	0.377	0.076	-0.034

Variable	Communality	Factor	Eigenvalue	% Variation	Cum.%
Quartz	0.52	1	3.014	63.6	63.6
Feldspar	0.46	2	1.122	23.7	87.2
Porosity	0.78	3	0.388	8.2	95.4
Rock Fragments	0.60	4	0.167	3.5	98.8
Calcite	0.86	5	0.050	1.1	100.0
Siderite	0.98				
Matrix	0.53				

TABLE A5

R-Mode Factor Analysis
Upper Weir Samples

Factor Matrix Using Principal Factor With Iterations

	Factor 1	Factor 2	Factor 3	Factor 4	Factor 5
Quartz	0.708	-0.180	0.531	-0.118	0.089
Feldspar	0.232	0.808	-0.285	0.314	0.320
Porosity	0.524	0.725	0.119	0.175	-0.271
Rock Fragments	0.485	-0.738	-0.159	0.277	0.171
Calcite	-0.868	-0.090	0.302	0.360	-0.047
Siderite	-0.858	0.199	0.068	-0.159	0.150
Matrix	0.045	0.241	0.562	0.046	0.191

Variable	Communality	Factor	Eigenvalue	% Variation	Cum. %
Quartz	0.84	1	2.56	49.4	49.4
Feldspar	0.90	2	1.86	30.5	79.9
Porosity	0.92	3	0.81	12.5	92.8
Rock Fragments	0.91	4	0.29	4.8	97.6
Calcite	0.98	5	0.27	2.4	100.0
Siderite	0.82				
Matrix	0.42				

TABLE A6

R-Mode Factor Analysis
Lower Weir Samples

Factor Matrix using Principal Factor with Iterations

	Factor 1	Factor 2	Factor 3	Factor 4	Factor 5
Quartz	0.659	0.132	-0.480	-0.105	0.032
Feldspar	0.526	0.111	0.079	0.447	0.127
Porosity	0.248	0.575	0.301	-0.098	-0.027
Rock Fragments	0.842	-0.009	0.189	-0.097	0.139
Calcite	-0.871	-0.080	-0.081	0.195	0.086
Siderite	-0.961	0.271	0.064	-0.130	0.065
Matrix	0.180	-0.789	0.174	-0.080	-0.005

Variable	Communality	Factor	Eigenvalue	% Variation	Cum %
Quartz	0.69	1	3.20	65.1	65.1
Feldspar	0.49	2	1.03	20.0	85.1
Porosity	0.49	3	0.40	7.7	92.8
Rock Fragments	0.77	4	0.29	6.5	99.3
Calcite	0.81	5	0.03	0.7	100.0
Siderite	0.99				
Matrix	0.69				

APPENDIX B1
Point Count Data
Core MCD 539
(in %)

Sample Number	Quartz	Feldspar	MRFs	SRFs	Calcite	Siderite	Sulfate
RP1	52	7	5	15	1	0	0
RP2	55	6	4	12	2	0	0
RP3	57	5	3	14	3	0	0
RP4	55	5	5	13	3	0	0
RP5	56	8	6	11	2	1	0
RP6	55	4	5	14	2	0	0
RP7	55	4	8	15	4	0	0
RP8	55	5	5	12	3	1	0
RP9	57	4	4	17	3	0	0
RP10	56	4	4	14	6	7	0
RP11	59	4	5	13	3	9	0
RP12	58	4	5	14	4	2	0
RP13	58	5	3	14	4	3	0
RP14	Shale						

APPENDIX B1
Point Count Data
Core MCD 539

Sample Number	Accessory Minerals	Matrix	Point Count Porosity	Core Lab Porosity	Pyrite
RP1	1	3	15	11.6	0
RP2	1	6	13	12.5	0
RP3	1	4	12	13.2	0
RP4	1	3	15	12.4	0
RP5	1	2	13	12.5	0
RP6	1	3	15	10.4	1
RP7	1	4	6	10.0	1
RP8	1	4	9	11.3	2
RP9	1	5	7	10.0	2
RP10	1	2	6	6.0	0
RP11	1	2	4	6.0	0
RP12	0	6	7	6.0	0
RP13	1	8	8	6.0	0
RP 14	Shale				

APPENDIX B2
Point Count Data
Core MCD 543

Sample Number	Accessory Minerals	Matrix	Point Count Porosity	Core Lab Porosity	Pyrite
BP1	1	4	15	11.8	0
BP2	1	4	14	11.4	0
BP3	0	3	17	10.8	0
BP4	2	2	16	11.5	0
BP5	1	3	13	10.7	0
BP6	1	4	15	9.6	0
BP7	1	6	9	9.7	0
BP8	Shale				
BP9	2	7	5	7.3	2
BP10	2	10	4	6.4	5
BP11	1	8	1	4.0	2
BP12	1	12	0	0	3
BP13	0	7	0	0	1
BP14	1	10	0	0	2
BP15	0	10	0	1.7	1
BP16	1	9	2	2.3	3
BP17	1	8	0	5.7	1
BP18	0	6	0	1.6	2
BP19	0	4	0	1.6	1
BP20	1	3	0	0.8	0
BP21	1	3	0	0	0

APPENDIX B2
Point Count Data
Core MCD 543
(in %)

Sample Number	Quartz	Feldspar	MRFs	SRFs	Calcite	Siderite	Sulfate
BP1	54	5	6	10	5	0	0
BP2	56	7	4	11	3	0	0
BP3	53	5	6	14	2	0	0
BP4	53	7	4	13	2	1	0
BP5	49	5	5	12	7	5	0
BP6	48	5	6	10	5	6	0
BP7	51	5	4	8	6	10	0
BP8	Shale						
BP9	55	5	6	14	3	0	0
BP10	53	4	6	15	1	0	0
BP11	53	5	7	18	4	1	0
BP12	54	5	6	15	3	1	0
BP13	48	4	4	10	8	18	0
BP14	55	3	4	14	5	6	0
BP15	54	5	6	12	7	4	1
BP16	53	5	5	14	6	1	1
BP17	42	4	4	8	8	24	0
BP18	56	5	4	12	6	7	2
BP19	52	3	3	12	14	4	7
BP20	52	3	4	10	15	12	0
BP21	48	3	3	11	26	6	0

APPENDIX C

CLAY ABUNDANCE

Sample Number	Kaolinite	Illite	Chlorite	Porosity (%)
BP1	3.5	1.4	1.1	11.8
BP3	2.6	2.1	1.0	10.8
BP5	3.5	1.5	1.5	10.7
BP7	1.7	2.4	0.7	9.7
BP8	0.5	7.7	0.3	0.0
BP9	0.7	0.9	0.4	7.3
BP10	1.9	2.8	0.5	6.4
BP12	0.6	3.7	0.5	0.0
BP13	0.8	1.6	0.4	0.0
BP15	0.6	1.7	0.4	1.7
BP16	0.7	0.6	0.3	2.3
BP17	0.8	1.8	0.3	5.7
BP19	0.9	0.9	0.5	1.6
BP20	0.9	0.8	0.4	0.8

Sample Number	Kaolinite	Illite	Chlorite	Porosity(%)
RP1	3.6	1.9	1.2	11.6
RP3	3.6	1.3	1.3	13.2
RP5	2.8	1.9	1.0	12.5
RP7	1.7	2.4	0.6	10.0
RP9	1.7	3.3	0.7	10.0
RP11	1.9	1.9	0.5	6.0
RP12	3.1	2.2	0.9	6.0
RP13	3.6	1.3	1.8	6.0

Unitless values of clay abundance derived XRD patterns using the semi-quantitative method of Thorez(1976). Porosity values are from Core Laboratory Hg injection test.